I&EC research
Industrial & Engineering Chemistry Research

Article

pubs.acs.org/IECR

Ethylene Glycol and Its Mixtures with Water and Electrolytes: Thermodynamic and Transport Properties

Peiming Wang,* Jerzy J. Kosinski, Andrzej Anderko, Ronald D. Springer, Malgorzata M. Lencka, and Jiangping Liu

OLI Systems, Inc., 240 Cedar Knolls Road, Suite 301, Cedar Knolls, New Jersey 07927, United States

Supporting Information

ABSTRACT: A comprehensive thermodynamic model has been developed for calculating thermodynamic and transport properties of mixtures containing monoethylene glycol (MEG), water, and inorganic salts and gases. The model is based on the previously developed mixed-solvent electrolyte (MSE) framework, which has been designed for the simultaneous calculation of phase equilibria and speciation of electrolytes in aqueous, nonaqueous, and mixed solvents up to the saturation or pure solute limit. In the MSE framework, the standard-state properties of species are calculated from the Helgeson−Kirkham−Flowers equation of state, whereas the excess Gibbs energy includes a long-range electrostatic interaction term expressed by a Pitzer−Debye−Hückel equation, a virial coefficient-type term for interactions between ions and a short-range term for interactions involving neutral molecules. Model parameters have been established to reproduce the vapor pressures, solubilities of solids and gases, heat capacities, and densities for MEG + H_2O + solute systems, where the solute is one or more of the following components: NaCl, KCl, $CaCl_2$, Na_2SO_4, K_2SO_4, $CaSO_4$, $BaSO_4$, Na_2CO_3, K_2CO_3, $NaHCO_3$, $KHCO_3$, $CaCO_3$, HCl, CO_2, H_2S, and O_2. In particular, emphasis has been put on accurately representing the solubilities of mineral scales, which commonly appear in oil and gas environments. Additionally, the model predicts the pH of mixed-solvent solutions up to high MEG contents. On the basis of speciation obtained from the thermodynamic model, the electrical conductivity of the MEG + H_2O + NaCl + $NaHCO_3$ solutions is also calculated over wide ranges of solvent composition and salt concentration. Additionally, associated models have been established to compute the thermal conductivity, viscosity, and surface tension of aqueous MEG mixtures.

1. INTRODUCTION

Ethylene glycol is an important industrial solvent and raw material in a variety of processes. In the oil and gas industries, monoethylene glycol (MEG) is commonly used to reduce the risk of gas hydrate formation during the production and transportation of hydrocarbons because gas hydrates pose serious economic and safety problems by blocking pipelines or plugging up wells and preventing gas production.[1] At the same time, organic gas hydrate inhibitors such as MEG may cause adverse scaling phenomena in drilling fluids and produced water, which commonly contain high concentrations of dissolved minerals. Therefore, the thermodynamic behavior of MEG-containing systems directly affects gas hydrate and scale control, which are two of the key aspects of flow assurance in the petroleum industry. In addition, the presence of important gas contaminants such as CO_2, H_2S, and O_2 in crude oil and natural gas processing requires the knowledge of their solubilities in fluids that may contain ethylene glycol. Moreover, ethylene glycol is used as an antisolvent or an additive in crystallization to obtain solid materials of desirable physical quality and chemical purity.[2,3] Therefore, a better understanding of salting-out effects and solubility behavior is necessary for the effective design and implementation of optimum operating conditions and equipment for processes involving such complex systems. Accurate models are thus clearly of vital importance to predict the phase and chemical behavior as well as other relevant thermophysical properties of MEG-containing systems.

Because of the practical importance of MEG, a large number of research papers has been published in the literature about systems containing aqueous MEG, various salts, and dissolved gases. The reported studies include data on phase equilibria,[4−50] speciation,[26,51,52] caloric effects,[53,54] densities,[11,12,53,55−57] surface tension,[33,58−62] and transport properties such as viscosity and electrical and thermal conductivity.[31,53,54,63−70] These data make it possible to develop comprehensive thermodynamic and transport property models for the simulation of chemical processes in which MEG plays a role. The recent work of Fosbøl et al.[71] on modeling the system MEG + water + CO_2 + Na_2CO_3 + $NaHCO_3$ represents an important advancement in the understanding and simulation of such systems but is limited to carbonates and bicarbonates as salt components.

Modeling phase equilibria in MEG-containing systems requires the use of a comprehensive thermodynamic model for mixed-solvent electrolyte mixtures. At the same time, it is highly desirable to have a computational framework that can be used for predicting transport properties and surface tension as well as bulk-phase thermodynamic properties. Besides its obvious practical usefulness, such a framework would provide additional insights into the properties of such systems. For example, when analyzing transport phenomena (e.g., electrical

Received: June 19, 2013
Revised: October 10, 2013
Accepted: October 14, 2013
Published: October 14, 2013

dx.doi.org/10.1021/ie4019353 | *Ind. Eng. Chem. Res.* 2013, 52, 15968−15987

and thermal conductivity, viscosity, and diffusivity), the ionization behavior of electrolytes in MEG-water mixtures needs to be taken into account. Thus, a reasonable prediction of speciation is important for the simultaneous representation of phase equilibria and transport properties.

In this study, we first apply a previously developed speciation-based thermodynamic model,[72,73] referred to as the MSE (mixed-solvent electrolyte) model, to selected MEG-containing systems with a particular focus on salts and gases that commonly exist in oilfield waters. The MSE model was previously shown to reproduce simultaneously vapor−liquid, solid−liquid, and liquid−liquid equilibria, speciation, caloric, and volumetric properties of electrolytes in water, organic, or mixed solvents.[74,75] In particular, the model is capable of reproducing solubility variations with solvent and ionic composition in crystallization studies[76] and accurately represents phase equilibria in multicomponent inorganic systems containing multiple salts, acids, bases,[74,77−84] and ionic liquids.[85] A combination of the MSE model and the extensive thermodynamic data that are available in the literature for MEG-containing systems provides an excellent opportunity for developing a comprehensive thermodynamic treatment. After establishing the parameters of the thermodynamic model, we develop associated models for electrical conductivity, thermal conductivity, viscosity, and surface tension.

2. THERMODYNAMIC FRAMEWORK

Details of the thermodynamic model have been described elsewhere.[73,75] Here, we briefly introduce the fundamentals of the model and specify the parameters that need to be determined on the basis of experimental data. The thermodynamic framework has been designed to provide a simultaneous treatment of phase equilibria, ionic equilibria in the solution, and derivative thermodynamic properties such as enthalpy and heat capacity. To achieve this objective, the framework consists of

(a) An excess Gibbs energy model that accounts for the nonideality of liquid systems containing ionic and neutral solute species in single or multicomponent solvents;
(b) A standard-state property model that determines the thermodynamic properties of individual species at infinite dilution and thus defines the reference state for constructing the solution nonideality model;
(c) Chemical equilibrium equations that account for acid−base equilibria (including the self-dissociation of water and MEG molecules) and the formation of ion pairs or other aqueous complexes; and
(d) A cubic equation of state for representing the properties of the gas phase.

The excess Gibbs energy is expressed as

$$\frac{G^{ex}}{RT} = \frac{G^{ex}_{LR}}{RT} + \frac{G^{ex}_{II}}{RT} + \frac{G^{ex}_{SR}}{RT} \tag{1}$$

where G^{ex}_{LR} represents the contribution of long-range electrostatic interactions, G^{ex}_{II} accounts for specific ionic (ion−ion and ion−molecule) interactions, and G^{ex}_{SR} is a short-range contribution resulting from intermolecular interactions. The long-range interaction contribution is calculated from the Pitzer−Debye−Hückel formula[86] expressed in terms of mole fractions and symmetrically normalized. The specific ion-interaction contribution is calculated from an ionic-strength-dependent, symmetrical second virial coefficient-type expression[73]

$$\frac{G^{ex}_{II}}{RT} = -\left(\sum_i n_i\right) \sum_i \sum_j x_i x_j B_{ij}(I_x) \tag{2}$$

where $B_{ij}(I_x) = B_{ji}(I_x)$, $B_{ii} = B_{jj} = 0$ and the ionic strength dependence of B_{ij} is given by

$$B_{ij}(I_x) = b_{ij} + c_{ij} \exp(-\sqrt{I_x + a_1}) \tag{3}$$

where b_{ij} and c_{ij} are adjustable parameters and a_1 is set equal to 0.01. The parameters b_{ij} and c_{ij} are calculated as functions of temperature as

$$b_{ij} = b_{0,ij} + b_{1,ij}T + b_{2,ij}/T + b_{3,ij}T^2 + b_{4,ij} \ln T \tag{4}$$

$$c_{ij} = c_{0,ij} + c_{1,ij}T + c_{2,ij}/T + c_{3,ij}T^2 + c_{4,ij} \ln T \tag{5}$$

For most electrolyte systems, only the first three terms are necessary to represent the variations of thermodynamic properties with temperature over a temperature range up to 300 °C. Additional temperature-dependent parameters are necessary only for a limited number of systems for which data analysis needs to be performed over an extended range of temperatures.[84] In cases where very high pressures are of interest, a pressure dependence may also be introduced into the b_{ij} and c_{ij} parameters.[84]

The short-range interaction contribution is calculated from the UNIQUAC equation.[87] When justified by experimental data, the temperature dependence of the UNIQUAC energetic parameters can be expressed using a quadratic function:

$$a_{ij} = a^{(0)}_{ij} + a^{(1)}_{ij}T + a^{(2)}_{ij}T^2 \tag{6}$$

In systems containing only strong electrolytes, only the specific ion-interaction parameters are needed to reproduce the properties of the solutions. However, in nonelectrolyte systems such as the MEG + water binary, only the short-range parameters are needed. For electrolyte systems such as those encountered in oilfield waters and brines where the ionic strength and salt concentrations are significant, the specific ion-interaction contribution is the most important one to reproduce the properties of the solutions. When a chemical process occurs in a mixed solvent or in solutions where undissociated inorganic acids or bases are present in significant amounts, the short-range contribution must be introduced to account for molecular interactions between the undissociated acid or base and the solvent molecules or between solvent components.

Although the excess Gibbs energy model is used to calculate nonideality effects on solution properties, the chemical equilibrium is governed by the chemical potentials of all species that participate in various reactions, such as precipitation, hydrolysis, and ion pairing. The chemical potential of each ionic or neutral species i is determined by its standard-state chemical potential, $\mu_i^0(T,P)$, and its activity coefficient, $\gamma_i(T,P,x)$. In other words

$$\mu_i(T, P, x) = \mu_i^0(T, P) + RT \ln x_i\gamma_i(T, P, x) \tag{7}$$

The standard-state chemical potentials of aqueous species, $\mu_i^0(T,P)$, are calculated as functions of temperature and pressure using the Helgeson−Kirkham−Flowers (HKF) equation of state.[88−90] The parameters of the HKF model are available for various aqueous species.[91−93] The standard-state properties

dx.doi.org/10.1021/ie4019353 | Ind. Eng. Chem. Res. 2013, 52, 15968−15987

Table 1. Literature Data Sources for the MEG + H_2O Binary System[a]

ref	type of data	T, K	P, atm	concentration range
Sokolov et al.[4]	VLE[b]	292−360	0.013−0.13	x = 0.19−0.99
Chiavone-Filho et al.[5]	VLE[c]	343, 363	P_{sat}	x = 0−0.86
Trimble and Potts[6]	VLE[b]	343−470	0.3−0.98	x = 0−1
Ogorodnikov et al.[7]	VLE[b]	373−470	1.0	x = 0−1
Gonzalez and Van Ness[8]	VLE[c]	323	P_{sat}	x = 0.02−0.98
Villamanan et al.[9]	VLE[c]	333	P_{sat}	x = 0−1
Curme[108]	VLE[c]	339−450	P_{sat}	x = 0−1
Horstmann et al.[109]	VLE[c]	333, 353	P_{sat}	x = 0−1
Daubert and Danner[110]	VLE	273−573	P_{sat}	x = 1
Cordray et al.[111]	SLE	217−273	1.0	x = 0−1
Ross[112]	SLE	220−273	1.0	x = 0−0.85
Liu et al.[113]	SLE	205−273	1.0	x = 0−0.38
Weast and Lide[114]	SLE	222−273	1.0	x = 0.001−0.3
Nan et al.[54]	C_p	273−373	1.0	x = 0−1
Yang et al.[53]	C_p, ρ, η	273−353	1.0	x = 0−1
Morénas and Douhéret[115]	ρ	288−308	1.0	x = 0−1
Hayduk and Malik[31]	ρ, η	298	1.0	x = 0−1
Sun and Teja[63]	ρ, η, λ	296−450	P_{sat}	x = 0.25−0.75 (to x = 1 for η)
Sesta and Berardelli[64]	ρ, η	298	1.0	x = 0.11−1
Iulian and Ciocîrlan[116]	ρ, η	293−313	1.0	x = 0−1
Egorov et al.[55]	ρ	278−333	1.0	x = 0−1
Lee and Hong[56]	ρ	283−303	1.0	x = 0.0083−0.87
Zhang et al.[57]	ρ	308−323	1.0	x = 0−1
Won et al.[33]	ρ, η, σ	298	1.0	x = 0−0.2
Horoibe et al.[62]	σ	253−298	1.0	x = 0−1
Habrdova et al.[60]	σ	298	1.0	x = 0.008−0.2
Hoke and Chen[61]	σ	298−471	P_{sat}	x = 0.047−1
Nakanishi et al.[59]	σ	303	1.0	x = 0−1
Kalies et al.[58]	σ	293	1.0	x = 0−1
Bogacheva et al.[69]	λ	298−363	1.0	x = 0−1
Assael et al.[68]	λ	296−355	1.0	x = 0.088−1
Bohne et al.[67]	ρ, η, λ	253−470	P_{sat}	x = 0−1
Vanderkooi et al.[66]	λ	273−373	1.0	x = 0−1
Usmanov and Salikhov[65]	λ	293	1.0	x = 0−1

[a]The symbol x denotes the mole fraction of MEG, ρ, density, η, viscosity, λ, thermal conductivity, and σ, surface tension. [b]Data determined under isobaric conditions. [c]Data determined under isothermal conditions.

calculated from the HKF model are based on the infinite-dilution reference state and on the molality concentration scale. To make the equilibrium calculations consistent when the standard-state properties are combined with the mole-fraction-based and symmetrically normalized activity coefficients, two conversions are performed.[73] (1) The activity coefficients calculated from eq 1 are converted to those based on the unsymmetrical reference state (i.e., at infinite dilution in water)

$$\ln \gamma_i^{x,*} = \ln \gamma_i^{x} - \lim_{\substack{x_i \to 0 \\ x_w \to 1}} \ln \gamma_i^{x} \tag{8}$$

where $\lim_{\substack{x_i \to 0 \\ x_w \to 1}} \ln\gamma_i^x$ is the value of the symmetrically normalized activity coefficient at infinite dilution in water, which is calculated by substituting $x_i = 0$ and $x_w = 1$ into the activity coefficient equations. (2) The molality-based standard-state chemical potentials are converted to corresponding mole-fraction-based quantities

$$\mu_i^{L,0,x}(T, P) = \mu_i^{L,0,m}(T, P) + RT \ln \frac{1000}{M_{H_2O}} \tag{9}$$

where M_{H_2O} is the molecular weight of water. The values of ln $\gamma_i^{x,*}$ and $\mu_i^{L,0,x}$ from eqs 8 and 9 are then used in eq 7 to determine the chemical potential of each species for chemical-equilibrium calculations. Thus, the calculations require the availability of parameters for both the standard-state properties and activity coefficients. For speciation calculations in non-aqueous or mixed-solvent electrolyte solutions, it is of interest to consider the change in the thermodynamic state of individual ions as they are moved from an aqueous to a mixed-solvent environment. This is significant because the Helgeson−Kirkham−Flowers equation defines the standard-state chemical potentials at infinite dilution in water and not in any other solvent. The difference between the chemical potential at infinite dilution in water and in a nonaqueous (in particular, mixed) solvent is accounted for by the Gibbs energy of transfer of an ion from water to a nonaqueous solvent.[73] In general, the Gibbs energy of transfer from solvent R to solvent S is related to the activity coefficients by

$$\Delta_{tr}G_i^0(\mathrm{R} \to \mathrm{S})_m = RT \ln \frac{\gamma_i^{x,*,\mathrm{S}} M_\mathrm{S}}{\gamma_i^{x,*,\mathrm{R}} M_\mathrm{R}} \tag{10}$$

dx.doi.org/10.1021/ie4019353 | Ind. Eng. Chem. Res. 2013, 52, 15968−15987

Table 2. Literature Data Sources for the MEG + H_2O + Solute (S) Systems

S	ref	type of data	T, K	P, atm	concentration range[a]
NaCl	Zhou et al.[11,12]	solubility	288−308	1	x' = 0−1, m_s
		density			x' = 0−1, m = 1−m_s
	Masoudi et al.[36]	solubility	273−348	1	x' = 0.031−0.16, m_s
		freezing point	252−270		x' = 0.018−0.058, m = 0.46−3.04
		boiling point	375−384		x' = 0.019−0.17, m = 0.94−2.65
	Kraus et al.[38]	solubility	298	1	x' = 0−1, m_s
	Isbin and Kobe[37]	solubility	298	1	x' = 1, m_s
	Trimble[14]	solubility	303	1	x' = 0−1, m_s
	Baldwin et al.[39]	solubility	323	1	x' = 0−1, m_s
	Kan et al.[27]	solubility	298	1	x' = 0−0.22, m_s
	Parrish[40]	solubility	273−289	1	x' = 0−0.11, m_s
	Parrish and Allred[41]	a_w	274−289	1	x' = 0.049 and 0.11, m = 0.9−5.1
	Woods et al.[21]	freezing point	214−273	1	x'=0−0.3, m = 0−4.3
	Sandengen and Kaasa[70]	electrical conductivity	298	1	x' = 0.1−1, m = 0−2.4
KCl	Zhou et al.[11,12]	solubility, ρ	288−308	1	x' = 0−1, m_s
	Masoudi et al.[36]	freezing point	252−271	1	x' = 0.0076−0.11, m = 0.4−2.2
		boiling point	374−385		x' = 0.015−0.29, m = 0.69−2.78
	Parrish[40]	solubility	273−289	1	x' = 0−0.11, m_s
	Trimble[14]	solubility	303	1	x' = 0−1, m_s
	Armstrong and Eyre[48]	solubility	298	1	x' = 0−0.018, m_s
	Chiavone and Rasmussen[49]	solubility	298−348	1	x' = 0.076−1, m_s
	Adavcová[16]	solubility	298	1	x' = 0.031−1, m_s
	Masoudi et al.[17]	solubility	298−348	1	x' = 0.19 and 0.63, m_s
$CaCl_2$	Isbin and Kobe[37]	solubility	298	1	x' = 1, m_s
	Parrish[40]	solubility	273−289	1	x' = 0−0.11, m_s
	Parrish and Allred[41]	a_w	274−289	1	x' = 0.044−0.11, m = 0.48−1.6
	Masoudi et al.[45]	solubility	273−303	1	x' = 0.031−0.16, m_s
		freezing point	253−270		x' = 0.013−0.092, m = 0.32−1.45
		boiling point	374−380		x' = 0.013−0.17, m = 0.32−1.45
K_2CO_3	Kobe and Stong[46]	solubility	298−313	1	x' = 0−1, m_s
K_2SO_4	Fox and Gauge[50]	solubility	298	1	x' = 0.01−0.22, m_s
	Trimble[14]	solubility	303	1	x' = 0−0.36, m_s
Na_2SO_4	Vener and Tompson[13]	solubility	298−408	1	x' = 0−0.97, m_s
$CaSO_4$	Kaasa et al.[26]	solubility	298−338	1	x' = 0−1, m_s
Na_2CO_3	Oosterhof et al.[30]	solubility	313−363	1	x' = 0−1, m_s
	Gärtner et al.[29]	solubility	313−363	1	x' = 0−1, m_s
$NaHCO_3$	Gärtner et al.[29]	solubility	288−363	1	x' = 0.22−1, m_s
	Sandengen and Kaasa[70]	electrical conductivity	298	1	x' = 0−1, m = 0−1
HCl	Gerrard and Macklen[42]	solubility/VLE	273−320	P_{HCl} = 1	x' = 1
	O'Brien et al.[44]	solubility/VLE	298	P_{HCl} = 0.0008−0.424	x' = 1, x_{HCl} = 0.076−0.353
O_2	Yamamoto and Tokunaga[22]	solubility/VLE	298	1	x' = 0−1
	Joosten et al.[47]	solubility/VLE	278−409	P_{o_2} = 0.21	x' = 0.22−1
H_2S	Jou et al.[24]	solubility	298−398	P_{H_2S} = 0.031−67	x' = 1
	Lenoir et al.[23]	Henry's law constant	298	low P_{H_2S}	x' = 1
	Gerrard[25]	solubility	265−293	P_{H_2S} = 1	x' = 1
	Short et al.[20]	solubility	263−333	P_{H_2S} = 1	x' = 1
CO_2	Byeseda et al.[28]	solubility	297	P_{CO_2} = 1	x' = 1
	Lenoir et al.[23]	solubility	298	P_{CO_2} = 0.1	x' = 1
	Hayduk and Malik[31]	solubility	298	P_{CO_2} = 1	x' = 0−1
	Kobe and Mason[32]	solubility	298	P_{CO_2} = 1	x' = 0−0.3
	Won et al.[33]	solubility	298	P_{CO_2} = 1	x' = 0−0.2

dx.doi.org/10.1021/ie4019353 | Ind. Eng. Chem. Res. 2013, 52, 15968−15987

Table 2. continued

S	ref	type of data	T, K	P, atm	concentration range[a]
	Oyevaar et al.[34]	solubility	298	P_{CO_2} = 1	x' = 0−1
	Jou et al.[24]	VLE	298−398	0.29−200	x' = 1, x_{CO_2}=0.00069−0.139
	Kaminishi et al.[35]				x' = 1
$CaCl_2$ + NaCl	Parrish and Allred[41]	a_w solubility	273−289	1	x' = 0.049−0.11, m_{NaCl} = 0.72−2.4, m_{CaCl_2} = 0.095−0.32
					x' = 0−0.11, m_{CaCl_2} = 0.94−4.5, m_{NaCl} = m_s
$CaSO_4$ + NaCl	Kaasa et al.[26]	solubility	298−358	1	x' = 0−1, m_{NaCl} = 0.1, 0.5, 0.7, m_{CaSO_4} = m_s
$BaSO_4$ + NaCl	Kan et al.[27]	solubility	298	1	x' = 0−0.41, m_{NaCl} = 1 and 3 mol/kg H_2O, m_{BaSO_4} = m_s
	Parrish[40]	solubility	298	1	x' = 0−0.18, m_{NaCl} = 1 and 3 mol/kg H_2O, m_{BaSO_4}=m_s
$NaHCO_3$ + NaCl	Sandengen and Kaasa[70]	electrical conductivity	298	1	x' = 0−1, m_{NaCl} = 0−1, m_{NaHCO_3} = 0.1 and 0.25
$NaHCO_3$ + CO_2	Sandengen et al.[51]	pH	277−353	P_{CO_2} = 0.71−1	x' = 0.30 and 0.72, m_{NaHCO_3} = 0−0.96
	Kaasa et al.[26]	solubility, pH	298	P_{CO_2} ∼1	x' = 0−1, m_{NaHCO_3}=m_s
$KHCO_3$ + CO_2	Sandengen et al.[51]	pH	298	P_{CO_2} = 1	x' = 0.30 and 0.72, m_{KHCO_3} = 0−1.72
$NaHCO_3$ + NaCl + CO_2	Kaasa et al.[26]	solubility, pH	298−353	P_{CO_2} = 0.54−1	x' = 0−1, m_{NaCl} = 0.1, 0.5, 0.7, m_{NaHCO_3} = m_s
$CaCO_3$ + NaCl + CO_2	Kaasa et al.[26]	solubility, pH	298−353	P_{CO_2} = 0.58−1	x' = 0−0.85, m_{NaCl} = 0.1, 0.5, 0.7, m_{CaCO_3} = m_s

[a]The symbol x' denotes the mole fraction of MEG on a salt-free basis; x' = 1 if no water is present. m_s is the saturation molality in mol (kg solvent)$^{-1}$.

where M_Y (Y = S or R) are the molecular weights of solvent Y and $\gamma_i^{x,*,Y}$ is the mole-fraction-based unsymmetrical activity coefficient of ion i in solvent Y. Thus, with an appropriately constrained activity coefficient model, the Gibbs energies of transfer can be reproduced, and the model can be based on an infinitely dilute reference state in water even when water is not the only solvent.

For the species in the gas phase, the fugacity coefficients used to determine their chemical potentials have been calculated using the Soave−Redlich−Kwong (SRK) equation of state.[94,95]

On the basis of the chemical potentials calculated from eq 7, equilibrium expressions are written for ionic equilibria between solution species (i.e., for acid−base and ion-pairing reactions) and for phase equilibria (VLE and SLE). These expressions are solved together with material balance and electroneutrality constraints as discussed by Zemaitis et al.[96] and Rafal et al.[97]

3. TRANSPORT AND SURFACE PROPERTY MODELS

Models for transport and interfacial properties in aqueous and mixed-solvent electrolyte systems have been described previously.[98−107] In particular, models are available for calculating thermal and electrical conductivity, self-diffusivity, viscosity, and surface (L−V) and interfacial (L−L) tension over wide ranges of temperature, solvent composition, and electrolyte concentration. These models are coupled with the MSE thermodynamic framework to obtain the concentrations of individual ions, neutral molecules, complexes, and ion pairs that are used as input for the calculation of the transport and interfacial properties. The transport and interfacial property models have been designed to have the same applicability range as that of the MSE thermodynamic model (i.e., they can be applied to aqueous solutions ranging from infinite dilution to solid saturation or pure solute limit). They are equally applicable to nonelectrolyte mixtures and nonaqueous or mixed-solvent electrolyte systems. In the present work, the thermal conductivity, viscosity, and surface-tension models are applied to the MEG + water binary system, and the electrical conductivity model is used for selected MEG + water + salt systems. Details of these models can be found elsewhere,[98−101] and a brief summary of the relevant equations and associated parameters is given in the Supporting Information.

4. EVALUATION OF MODEL PARAMETERS

The MSE thermodynamic framework has been applied to model the phase behavior and other thermodynamic properties of the binary system MEG + H_2O and the mixed systems MEG + H_2O + solute, where the solute is one or more of the following components: NaCl, KCl, $CaCl_2$, Na_2SO_4, K_2SO_4, $CaSO_4$, $BaSO_4$, Na_2CO_3, K_2CO_3, $NaHCO_3$, $KHCO_3$, $CaCO_3$, HCl, CO_2, H_2S, and O_2. Model parameters for aqueous binary and multicomponent systems containing chloride salts (i.e., NaCl, KCl, and $CaCl_2$) and CO_2 have been reported in previous studies.[78,95] For other aqueous binary and multicomponent systems (i.e., those other than the chloride and CO_2 systems), ion-interaction parameters have been determined on the basis of analogous procedures and are used here as a foundation for modeling the MEG + H_2O + solute systems.

Tables 1 and 2 summarize the primary literature sources that were used for developing the model for MEG-containing systems together with their ranges of temperature, pressure, solvent composition, and salt content. The model parameters have been determined using thermodynamic data of various types (i.e., (1) vapor−liquid equilibria (VLE), (2) water activity (a_w), (3) solubilities of solids in MEG + H_2O mixtures and in pure MEG, including the melting point of MEG and freezing point data, (4) speciation data as exemplified by pH measurements, (5) volumetric data, and (6) caloric data such as heat capacities). The use of multiple data types is important to ensure the physical validity and accuracy of model parameters. For example, caloric data are useful to determine the temperature dependence of model parameters. This makes it possible to make reliable predictions of solubilities well beyond the temperature range of experimental data.

Prior to modeling multicomponent systems, model parameters have been developed for the MEG + H_2O binary. These parameters as well as those for aqueous salt systems provide a basis for modeling the properties of mixed systems containing salts and gaseous components in addition to MEG. Although

dx.doi.org/10.1021/ie4019353 | Ind. Eng. Chem. Res. 2013, 52, 15968−15987

Table 3. Model Parameters for the MEG + H_2O System: Standard-State Thermochemical Properties for Nonionized MEG Species in Various Phases and UNIQUAC Interaction Parameters[a]

Standard-State Properties at Infinite Dilution in Water						
species	$\Delta\overline{G}_f^0$, kJ mol^{-1}		$\overline{S}^0$, J mol^{-1}K^{-1}			
MEG(aq)	−334.660		248.97			
Pure-Component Liquid-Phase Properties						
	Cp (J mol^{-1} K^{-1}) = A + BT + CT^{2b}					
species	A	B	C			
MEG^0	35.54	0.43678	-1.8486×10^{-4}			
Solid-Phase Properties						
species	$\Delta_f G^\circ$, kJ mol^{-1}	S°, J mol^{-1} K^{-1}	C_p^0, J mol^{-1} K^{-1c}			
MEG(s)	−321.197	173.66	96.23			
MEG·H_2O	−559.297	222.87	138.07			
Henry's Law Constant						
	Log K = A + B/T + CT + DT^2					
equilibrium	A	B	C	D		
MEG(g) = MEG(aq)	−12.68451	4532.912	1.338141×10^{-2}	-5.897575×10^{-6}		
Binary Interaction Parameters						
	$a_{ij} = a_{ij}^{(0)} + a_{ij}^{(1)}\,T + a_{ij}^{(2)}\,T^2$					
species i	species j	$a_{ij}^{(0)}$	$a_{ij}^{(1)}$	$a_{ij}^{(2)}$	$a_{ji}^{(0)}$	$a_{ji}^{(1)}$	$a_{ji}^{(2)}$
MEG(aq)	H_2O	195.6597	−17.72271	2.244026×10^{-2}	−212.5369	31.50075	-5.463013×10^{-2}

[a]Parameters were determined in this study unless otherwise noted. [b]C_p equation coefficients were taken from Daubert and Danner.[110] The enthalpy and heat capacity of MEG + H_2O mixtures are calculated using a previously described methodology that utilizes the pure liquid heat capacity and its temperature dependence.[73] [c]C_p values for MEG(s) and MEG·H_2O were estimated according to Kubaschewski and Ünal.[128]

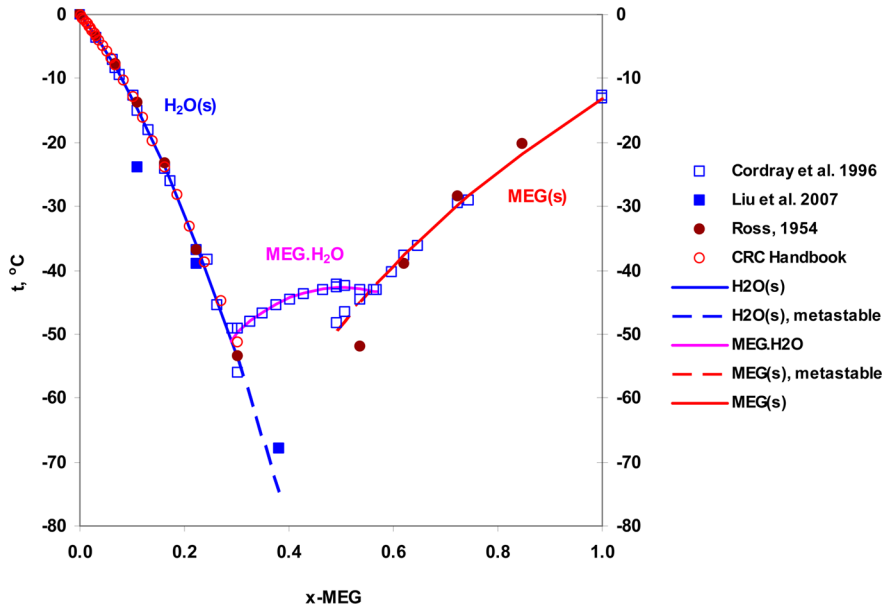

Figure 1. Comparison of the experimental (symbols) and calculated (curves) solid−liquid equilibria for the MEG + H_2O system. Experimental data were taken from Cordray et al.,[111] Liu et al.,[113] Ross,[112] and Weast and Lide.[114] The calculated results were obtained using the parameters given in Table 3.

the fundamental ions and ion pairs are the same in aqueous and MEG-containing systems, modeling the behavior of mixtures of MEG and inorganic components has revealed the need to introduce parameters that reflect the specific physical nature of such systems. This includes accounting for ion-pair formation and virial-type ion interactions involving the charged species and MEG.

The thermodynamic model is also used to provide speciation input for the calculation of transport and surface properties. This is especially important for the systems that contain salts because chemical speciation and ionic equilibria have a significant effect on transport properties in mixed solvents such as MEG + H_2O. Specifically, the electrical conductivity in the systems MEG + H_2O + NaCl, MEG + H_2O + $NaHCO_3$, and MEG + H_2O + NaCl + $NaHCO_3$ as well as the thermal conductivity, viscosity, and surface tension in the MEG + H_2O binary mixture has been examined. The experimental data that were used to evaluate the transport property and surface-tension parameters are also listed in Tables 1 and 2.

dx.doi.org/10.1021/ie4019353 | Ind. Eng. Chem. Res. 2013, 52, 15968−15987

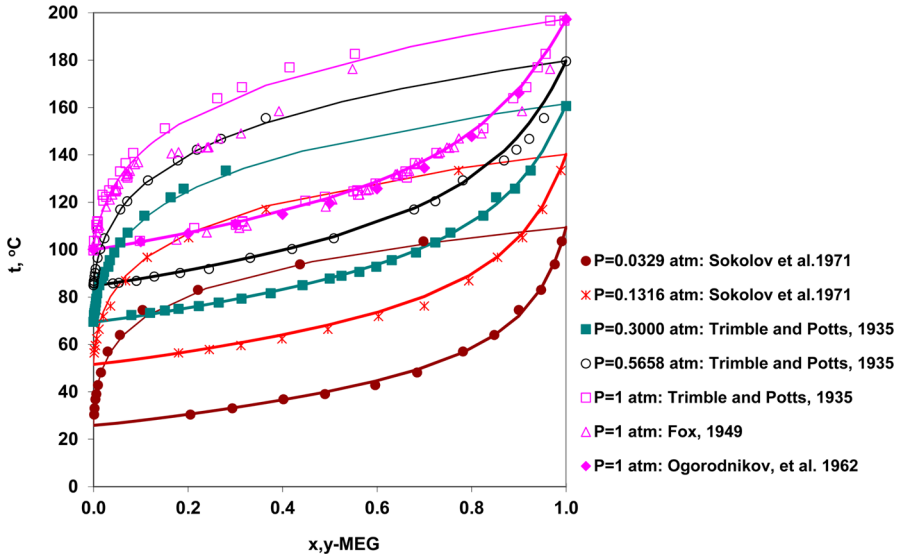

Figure 2. Vapor−liquid equilibria for the MEG + H_2O system at various pressures. The symbols are taken from the literature,[4,6,7,10] and the lines are calculated from the MSE model using the parameters given in Table 3.

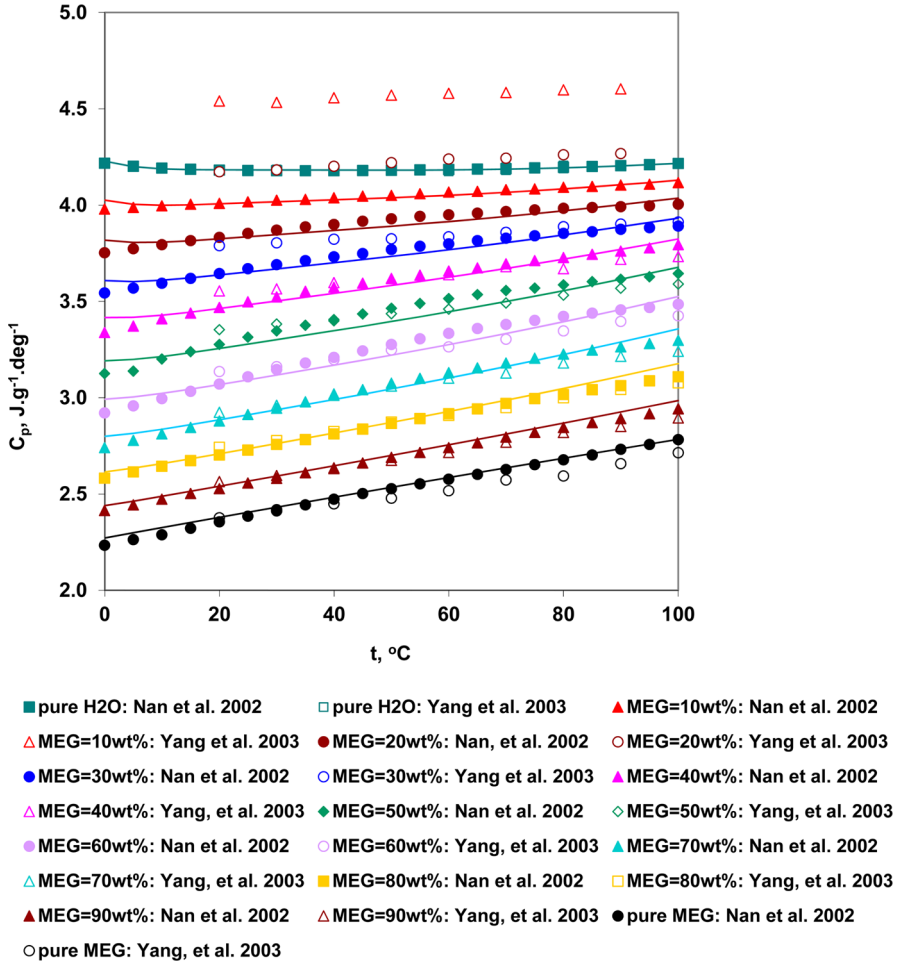

Figure 3. Heat capacities of liquid mixtures of MEG + H_2O as a function of temperature and composition. The symbols are taken from the literature,[53,54] and the lines are calculated from the MSE model using the parameters given in Table 3.

5. RESULTS AND DISCUSSIONS

Binary System MEG + H_2O. Extensive phase-equilibrium data are available in the literature for the MEG + H_2O system.[4−9,108−114] These data include vapor−liquid equilibrium, solubility, and freezing point measurements. Heat capacities and densities have also been extensively reported.[31,33,53−57,63,64,67,115,116] In addition to the thermodynamic properties, a considerable amount of data is available for

dx.doi.org/10.1021/ie4019353 | Ind. Eng. Chem. Res. 2013, 52, 15968−15987

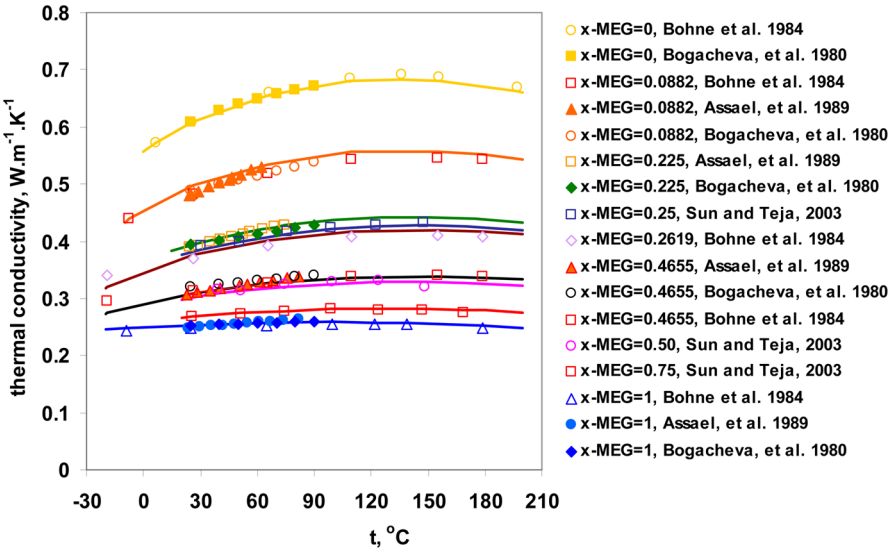

Figure 4. Thermal conductivity of liquid mixtures of MEG + H_2O as a function of temperature and composition. The symbols are taken from the literature,[63,67−69] and the lines are calculated from the thermal conductivity model[98] using the parameters given in Table S1.

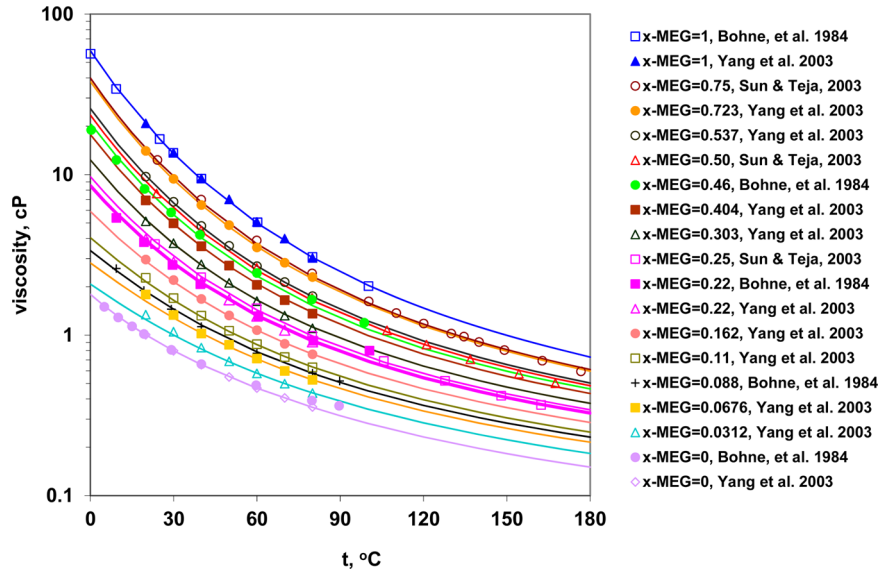

Figure 5. Viscosity of liquid mixtures of MEG + H_2O as a function of temperature and composition. The symbols are taken from the literature,[53,63,67] and the lines are calculated from the viscosity model[99] using the parameters given in Table S1.

the thermal conductivity, viscosity, and surface tension of the binary mixture as well as of pure liquid MEG. As shown in Table 1, the literature data span wide ranges of temperature and composition for this system and provide a comprehensive foundation for the determination of model parameters.

Modeling the thermodynamic properties of the binary system requires a simultaneous regression of all types of available data so that a consistent set of model parameters can be determined to represent multiple properties. Only the short-range interaction contribution to the excess Gibbs energy (i.e., the UNIQUAC term) is necessary to describe the nonideality of the binary MEG + H_2O mixture. The UNIQUAC parameters are temperature-dependent, as defined by eq 6. Table 3 lists the model parameters that reproduce the thermodynamic properties of this system. In addition to the UNIQUAC interaction parameters between MEG and H_2O, the standard-state properties (ΔG_f^0, S^0, and C_p^0) of MEG in the vapor, aqueous, and solid phases are also necessary. In particular, the standard-state chemical potentials of MEG in the liquid and vapor phases are intrinsically related to the Henry's law constant, which determines the vapor−liquid equilibria in conjunction with the UNIQUAC parameters. The standard-state chemical potential of MEG in the solid phase is needed to quantify the solubility and freezing point. The values of these standard-state properties have been adjusted, when necessary, together with the interaction parameters to obtain the best fit to the experimental data. The standard-state property values are also given in Table 3.

Selected results of modeling thermodynamic properties are shown in Figures 1−3 in which the calculated vapor−liquid and solid−liquid equilibria and heat capacities are compared with literature data. The freezing point data from several literature sources are generally consistent with each other[111−114] and are accurately represented from the freezing point of pure water to that of MEG (Figure 1). The solubility of an intermediate solid phase, identified as a monohydrate of MEG (i.e., MEG·

dx.doi.org/10.1021/ie4019353 | Ind. Eng. Chem. Res. 2013, 52, 15968−15987

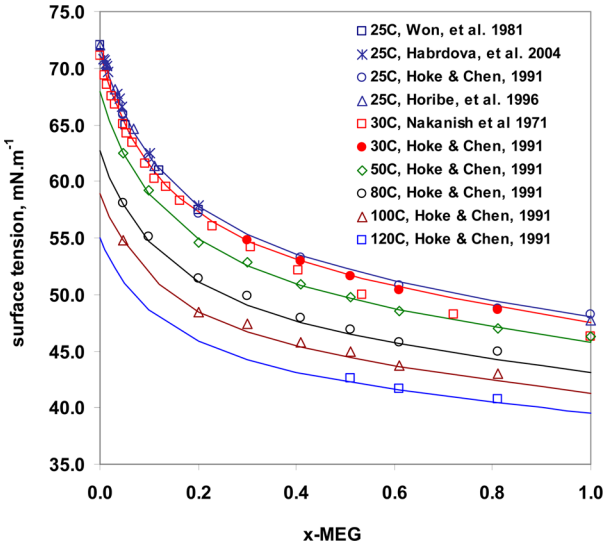

Figure 6. Surface tension of the MEG + H_2O system as a function of temperature and composition. The symbols are taken from the literature,[33,59−62] and the lines are calculated from the surface tension model[101] using the parameters given in Table S1.

H_2O),[111] is also accurately reproduced. Two distinct eutectic points appear in the phase diagram at the intersections of the MEG·H_2O solubility curve with those of pure MEG and ice. Vapor−liquid equilibria are also reproduced within the experimental uncertainty as shown in Figure 2. Figure 3 shows the heat capacity of MEG + H_2O mixtures at various compositions. The heat capacity data of Yang et al.[53] are significantly higher than those of Nan et al.[54] between the MEG mass fractions of 0.1 to 0.3 and show an unreasonable trend with MEG content. The data of Yang et al.[53] have not been used in the parametrization and are shown in Figure 3 only for comparison.

After establishing the thermodynamic parameters, the thermal conductivity, viscosity, and surface-tension model parameters have been developed for the MEG + H_2O mixtures. The model parameters are given in Table S1 in the Supporting Information, and the corresponding results are shown in Figures 4−6. For all three properties, the models represent the experimental data with a good accuracy across the full range of mole fractions and over a wide temperature range.

The parameters developed for the MEG + H_2O system provide a basis for modeling the effects of salts, acids, and dissolved gases. This will be discussed in the following sections.

MEG + H_2O + Salt Systems. The following systems have been analyzed:

(1) Ternary systems MEG + H_2O + S_1 (where S_1 is a single salt, i.e., S_1 = NaCl, KCl, $CaCl_2$, K_2CO_3, Na_2CO_3, $NaHCO_3$, K_2SO_4, Na_2SO_4, and $CaSO_4$)
(2) Ternary or binary systems MEG + S_1' with or without water (where S_1' is an acid or gas component, i.e., S_1' = HCl, CO_2, H_2S, and O_2)
(3) Quaternary systems MEG + H_2O + $MHCO_3$ + CO_2 (where M = Na or K) and MEG + H_2O + NaCl + S_1 (where S_1 = $CaCl_2$, $BaSO_4$, $CaSO_4$, and $NaHCO_3$)
(4) Quinary systems MEG + H_2O + MCO_3 + NaCl + CO_2 (where M = Ca or NaH).

These systems have been grouped together (with the exception of those containing H_2S and O_2) in the determination of model parameters because the prevailing aqueous species can be the same in the ternary, quaternary, and quinary systems, and, subsequently, the regressed binary interaction parameters may affect more than one of these systems. A simultaneous regression of data for these systems ensures the best accuracy of the parameters. The literature data that have been used in model development are summarized in Table 2. The model parameters that are necessary for reproducing the properties of all of the investigated systems are summarized in Tables 4−7. These parameters include the standard-state thermochemical properties of the aqueous ions, neutral species, and ion pairs (Table 4), the thermochemical properties of solids and gases (Table 5), and the binary interaction parameters between charged or uncharged aqueous species (Tables 6 and 7).

The solubilities of solid phases in nine ternary systems MEG + H_2O + S_1 are compared in Figure 7, where they are plotted as a function of the MEG mole fraction on a salt-free basis (i.e., x' MEG). For clarity, only the results at or near 25 °C are shown. The solubility of the salts decreases with MEG concentration in most of the systems. An exception is observed for the MEG +

Table 4. Standard-State Partial Molal Thermochemical Properties for Aqueous Ions, Neutral Species, and Ion Pairs[a,b]

species	$\Delta\bar{G}_f^0$, kJ mol^{-1}	$\bar{S}^0$, J mol^{-1}K^{-1}	$a_{HKF,1}$	$a_{HKF,2}$	$a_{HKF,3}$	$a_{HKF,4}$	$a_{HKF,1}$	$a_{HKF,2}$	ω
$C_2H_7O_2^+$	−317.368	254.2	0	0	0	0	0	0	0
$C_2H_5O_2^-$	−252.006	145.4	0	0	0	0	0	0	0
$C_2H_5O_2CO_2^-$	−665.477	254.5	0	0	0	0	0	0	0
$C_2H_5O_2HSO_4^{-2}$	−1063.802	145.7	0	0	0	0	−2.22744	0	0
H_2S(aq)[c]	−27.9198	125.52	0.65097	677.24	5.9646	−30 590	32.3	47 300	−10 000
O_2(aq)[c]	16.5435	108.951	0.57889	635.36	3.2528	−30 417	35.353	83 726	−39 430
$CaCO_3$(aq)[c]	−1099.61	41.2384	−0.03907	−873.25	9.1753	−24 179	−11.5309	−90641	−3800
$CaSO_4$(aq)[c]	−1311.00	27.5149	0.24079	−189.92	6.4895	−27 004	−8.4942	−81271	−100
$BaSO_4$(aq)	−1290.32	40.0043	0	0	0	0	110.8956	0	0
Ba^{2+c}	−560.782	9.6232	0.27383	−1005.65	−0.047	−23 633	3.8	−34 500	98 500
SO_4^{-2c}	−744.459	18.828	0.83014	−198.46	−6.2122	−26 970	1.64	−179 980	314 630
CO_3^{-2c}	−527.983	−49.9988	0.28524	−398.44	6.4142	−26 143	−3.3206	−171 917	339 140
HCO_3^{-c}	−586.940	98.4495	0.75621	115.05	1.2346	−28 266	12.9395	−47 579	127 330
HCl(aq)[d]	−87.4192	169.42	1.0217	0	0	0	16.1429	0	0

[a]Properties of CO_2(aq) and the species pertinent to the aqueous NaCl, KCl, and $CaCl_2$ solutions (i.e., Na^+, K^+, Ca^{2+}, $CaCl_2$(aq), and Cl^-) can be found in previous studies.[78,95] [b]Parameters were determined in this study unless otherwise noted. [c]Values were taken from Shock et al.[91,93] and Sverjensky et al.[92] [d]Parameters were determined in this study based on the properties of the HCl + H_2O system.

dx.doi.org/10.1021/ie4019353 | Ind. Eng. Chem. Res. 2013, 52, 15968−15987

Table 5. Pure-Component Parameters Used for Modeling Gas and Solid-Phase Properties[a]

			$C_p = a + bT + (c/T^2) + dT^2 + eT^3$				
species	ΔG_f^0, kJ mol^{-1}	S^0, J mol^{-1} K^{-1}	a	b	c	d	e
$H_2S_{(g)}$[b]	−33.440	205.59	25.9396	0.021954	162 922	9.08459×10^{-9}	-2.14101×10^{-9}
HCl(g)[b]	−95.300	186.901	30.0795	−0.006724	7858.39	1.2227×10^{-5}	-3.98114×10^{-9}
O_2(g)[b]	0	205.037	20.1541	0.028073	206 256	-1.7713×10^{-5}	4.17009×10^{-9}
$BaSO_4$(s)[c]	−1362.210	129.5958	126.6662	0.02071074	−2 291 430	7.4800×10^{-6}	0
$CaSO_4$(s)[c]	−1323.270	97.5587	113.05	0.0487	−2 481 000	0	0
$CaSO_4 \cdot 2H_2O$[c]	−1798.300	194.497	186.02	0	0	0	0
Na_2SO_4(s)[c]	−1269.950	146.6015	108.829	0.11008	−1 209 800	0	0
$Na_2SO_4 \cdot 10H_2O$[c]	−3646.940	585.6094	549.359	0	0	0	0
K_2SO_4(s)[c]	−1319.500	174.5276	96.9278	0.131099	−404 900	0	0
$CaCO_3$(s)[c]	−1128.870	89.8970	99.5462	0.027137	−2 148 100	0	0
$KHCO_3$(s)[c]	−867.538	117.9809	93.3032	0	0	0	0
$K_2CO_3 \cdot 1.5H_2O$[c]	−1431.480	198.8496	163.18	0	0	0	0
$NaHCO_3$(s)[c]	−850.913	108.8509	42.635	0.150875	0	0	0
Na_2CO_3(s)[c]	−1045.110	125.0836	64.1181	0.161604	0	0	0
$Na_2CO_3 \cdot H_2O$[c]	−1286.320	158.3033	145.6	0	0	0	0
$Na_2CO_3 \cdot 7H_2O$[c]	−2714.370	420.856	420	0	0	0	0
$Na_2CO_3 \cdot 10H_2O$[c]	−3427.700	566.1496	550.32	0	0	0	0

species	T_c, K[d]	P_c, atm[d]	ω[d]
H_2S(g)	373.53	88.457	0.0827
HCl(g)	324.69	82	0.126
O_2(g)	154.58	49.771	0.0218

[a]Properties of CO_2(g) and the solid phases in the NaCl + H_2O, KCl + H_2O, and $CaCl_2$ + H_2O systems can be found in previous work.[78,95] The properties of the MEG species (i.e., MEG(aq), MEG(s), MEG·H_2O, and MEG(g)) are listed in Table 3. [b]Values taken from the literature.[110,129,130] [c]The values of $\Delta_f G^o$ and S^0 were adjusted using solubility data in aqueous systems and the C_p values were taken from literature[131,132] or estimated[128,133] in this study. [d]Values taken from Daubert and Danner.[110]

Table 6. Binary Parameters Determined in This Study for Species Pairs Involving MEG

virial interaction parameters (eqs 4 and 5)[a]							
i	j	$b_{0,ij}$	$b_{1,ijj}$	$b_{2,ij}$	$c_{0,ij}$	$c_{1,ij}$	$c_{2,ij}$
MEG	CO_2(aq)	−3.158031	6.3015740×10^{-3}	0	−1.377927	0	0
MEG	HCl(aq)	−4.089249	0	2608.761	0	0	0
MEG	O_2(aq)	0	0	675.1891	0	0	0
MEG	$CaSO_4$(aq)	131.1763	0	−46828.3	0	0	0
MEG	Cl^-	−8.698285	0	983.2170	8.841474	0	0
MEG	CO_3^{-2}	−31.91460	3.8743210×10^{-2}	1354.314	0	0	5724.717
MEG	HCO_3^-	−6.747989	7.6135620×10^{-3}	2309.710	0	0	0
MEG	SO_4^{-2}	274.8513	−0.3963102	−52 938.59	−334.0798	0.4812396	62650.07
MEG	K^+	85.96771	−0.1205252	−13 474.76	−114.2762	0.1644379	17987.37
MEG	Na^+	6.048592	0	−439.2366	−6.004669	0	0
MEG	Ca^{2+}	−0.9709635	3.8602200×10^{-3}	0	0	0	0
MEG	Ba^{2+}	−35.32708	0	0	37.89691	0	0
MEG	$C_2H_7O_2^{+1}$	0	0	220.4113	0	0	0
$C_2H_7O_2^{+1}$	Cl^-	72.14760	0	−24808.38	0	0	0

UNIQUAC interaction parameters (eq 6)							
i	j	$a_{ij}^{(0)}$	$a_{ij}^{(1)}$	$a_{ij}^{(2)}$	$a_{ji}^{(0)}$	$a_{ji}^{(1)}$	$a_{ji}^{(2)}$
MEG	CO_2(aq)	−6211.478	22.11835	0	−177.2695	−9.520712	0
MEG	H_2S(aq)	−1584.588	0	0.0198533	7519.636	0	−0.04540988
MEG	O_2(aq)	90 609.00	−607.4458	1.055619	19005.08	−54.18313	−0.004384669
MEG	Cl^-	1521.117	0	0	2238.015	0	0
MEG	CO_3^{-2}	−76.02076	0	0	21893.94	0	0
MEG	HCO_3^-	5199.329	0	0	12611.04	0	0
MEG	SO_4^{-2}	−4271.487	0	0	16319.92	0	0
MEG	K^+	4949.462	0	0	5261.732	0	0
MEG	Na^+	−889.3011	0	0	11870.92	0	0

[a]For all of the species pairs, $b_{3,ij}$, $b_{4,ij}$, $c_{3,ij}$, $c_{4,ij}$ are set equal to zero.

dx.doi.org/10.1021/ie4019353 | Ind. Eng. Chem. Res. 2013, 52, 15968−15987

Table 7. Binary Parameters in the Virial Interaction (eqs 4 and 5) and UNIQUAC (eq 6) Terms for Species Pairs in the Aqueous Na_2SO_4, K_2SO_4, Na_2CO_3, K_2CO_3, $NaHCO_3$, $KHCO_3$, $CaCO_3$, $CaSO_4$, NaCl, H_2S, and HCl Systems.[a,b]

species i	species j		virial interaction parameters (eqs 4 and 5)
Na^+	SO_4^{-2}	$b_{0,ij}$, $b_{1,ij}$, $b_{2,ij}$, $b_{3,ij}$, $b_{4,ij}$	54 888.67, 25.45214, −1 320 671.0, -1.079190×10^{-2}, −10 023.51
		$c_{0,ij}$, $c_{1,ij}$, $c_{2,ij}$, $c_{3,ij}$, $c_{4,ij}$	−99 000.12, −45.46269, 2 404 424.0, 1.928067×10^{-2}, 18047.85
K^+	SO_4^{-2}	$b_{0,ij}$, $b_{1,ij}$, $b_{2,ij}$	242.3752, −0.3330860, −50 023.09
		$c_{0,ij}$, $c_{1,ij}$, $c_{2,ij}$	−491.1147, 0.7182240, 99 892.99
Na^+	HCO_3^-	$b_{0,ij}$, $b_{1,ij}$, $b_{2,ij}$	129.4830, −0.1780750, −23 932.30
		$c_{0,ij}$, $c_{1,ij}$, $c_{2,ij}$	−285.1680, 0.4076530, 49 974.90
K^+	HCO_3^-	$b_{0,ij}$, $b_{1,ij}$, $b_{2,ij}$, $c_{2,ij}$	−65.40770, 9.33473×10^{-2}, 10 980.10, 2380.890
Na^+	CO_3^{-2}	$b_{0,ij}$, $b_{1,ij}$, $b_{2,ij}$, $b_{3,ij}$	−185.2978, 0.7714720, 4695.440, -9.064150×10^{-4}
		$c_{0,ij}$, $c_{1,ij}$, $c_{2,ij}$, $c_{3,ij}$	141.7062, −0.9778970, 19 526.16, 1.469223×10^{-3}
K^+	CO_3^{-2}	$b_{0,ij}$, $b_{1,ij}$, $b_{2,ij}$	103.8650, −0.1272490, −29 244.10
		$c_{0,ij}$, $c_{1,ij}$, $c_{2,ij}$	−322.2640, 0.4641700, 71 799.40
$CaCO_{3(aq)}$	Cl^-	$b_{2,ij}$	2791.850
$CaCO_{3(aq)}$	Na^+	$b_{2,ij}$	2791.850
$CaSO_{4(aq)}$	Cl^-	$b_{0,ij}b_{1,ij}$, $b_{2,ij}$	205.0090, −0.2704200, −41 232.60
$CaSO_{4(aq)}$	Na^+	$b_{0,ij}$, $b_{1,ij}$, $b_{2,ij}$	−194.6930, 0.3360420, 28 460.40
Ca^{2+}	CO_3^{-2}	$b_{2,ij}$, $c_{2,ij}$	−155 596.0, 265 383.0
Ca^{2+}	HCO_3^-	$b_{0,ij}$, $b_{1,ij}$, $b_{2,ij}$	−287.8160, 0.5111480, 48 333.00
Ca^{2+}	SO_4^{-2}	$b_{0,ij}$, $b_{1,ij}$, $b_{2,ij}$	10887.73, −16.97345, −1 770 400
		$c_{0,ij}$, $c_{1,ij}$, $c_{2,ij}$	−15416.42, 24.21555, 2 508 590
CO_3^{-2}	Cl^-	$b_{0,ij}$, $b_{2,ij}$	0.8411780, 504.1941
HCO_3^-	Cl^-	$b_{0,ij}$, $b_{1,ij}$	−4.512144, 1.009086×10^{-2}
SO_4^{-2}	Cl^-	$b_{0,ij}$, $b_{1,ij}$, $b_{2,ij}$	−7.136240, 1.074150×10^{-2}, 1712.370
H_2S(aq)	H_2O	$b_{0,ij}$, $b_{1,ij}$, $b_{2,ij}$	−2.065078, 4.842357×10^{-3}, −40.59226
HCl(aq)	H_2O	$b_{0,ij}$, $b_{2,ij}$	1.191590, −908.5550
species i	species j		UNIQUAC interaction parameters (eq 6)
H_2S(aq)	H_2O	$a_{ij}^{(0)}$, $a_{ij}^{(1)}$, $a_{ij}^{(2)}$	7827.599, 7.095730, $-5.275172 \times 10^{-02}$
		$a_{ji}^{(0)}$, $a_{ji}^{(1)}$, $a_{ji}^{(2)}$	−14426.17, 69.10985, $-5.540216 \times 10^{-02}$
HCl(aq)	Cl^-	$a_{ij}^{(0)}$	−5536.390

[a]Parameters pertaining to the aqueous NaCl, KCl, $CaCl_2$, and CO_2 solutions can be found in previous studies.[78,95] [b]Parameters were determined on the basis of multiple properties in the aqueous binary systems of Na_2SO_4, K_2SO_4, Na_2CO_3, K_2CO_3, $NaHCO_3$, $KHCO_3$, $CaCO_3$, $CaSO_4$, H_2S, and HCl as well as selected ternary and quaternary systems with like ions (i.e., {CO_3^{-2}, Cl^-}, {HCO_3^-, Cl^-}, {SO_4^{-2}, Cl^-}).

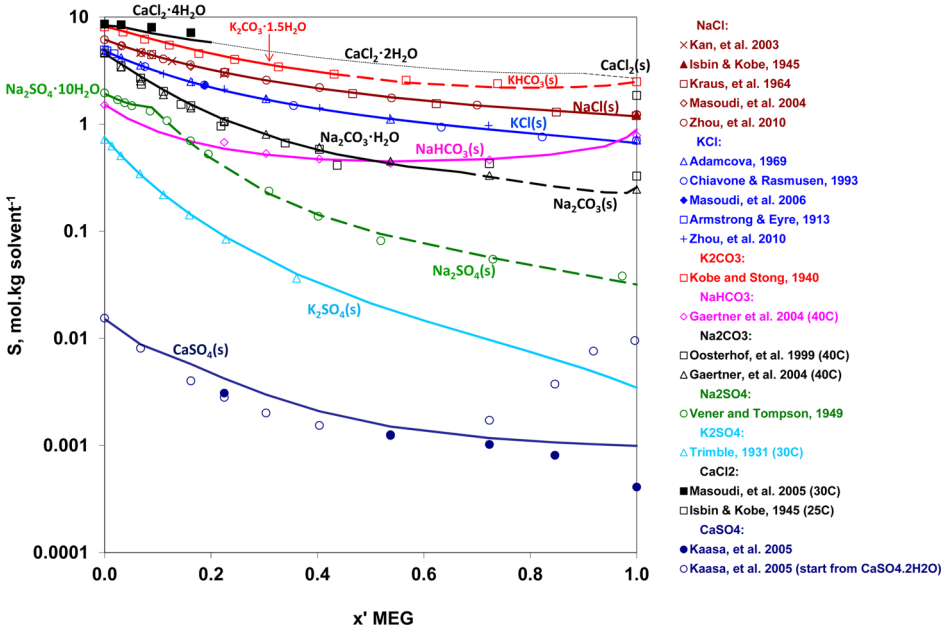

Figure 7. Comparison of the solubilities of salts in the MEG + H_2O + S system (S═NaCl, KCl, K_2CO_3, $CaCl_2$, Na_2CO_3, $NaHCO_3$, K_2SO_4, Na_2SO_4, and $CaSO_4$) at or near 25 °C as a function of solvent composition expressed as the mole fraction of MEG on a salt-free basis, x' MEG. The literature data (symbols) are listed in the legend. The solid phases are indicated next to the equilibrium lines where they precipitate. The lines are calculated from the MSE model using the parameters given in Tables 3−7.

dx.doi.org/10.1021/ie4019353 | Ind. Eng. Chem. Res. 2013, 52, 15968−15987

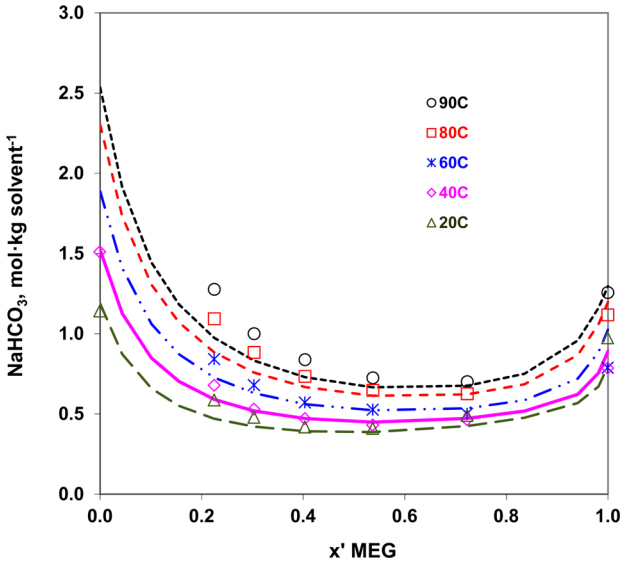

Figure 8. Solubility of $NaHCO_3(s)$ in MEG + H_2O mixtures at various temperatures as a function of solvent composition. The symbols are the experimental data from Gärtner et al.,[29] and the lines are calculated using the MSE model with parameters listed in Tables 3−7.

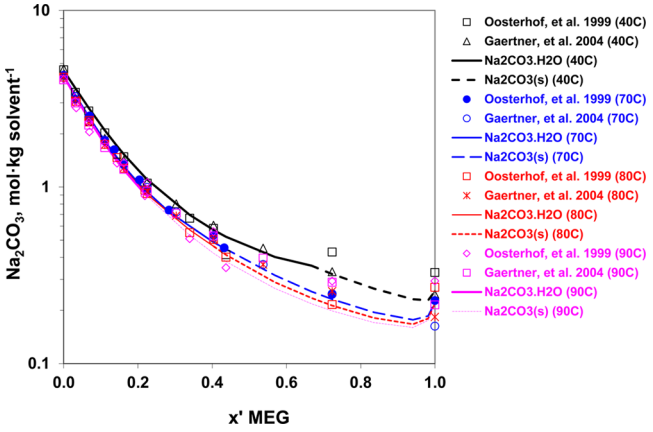

Figure 9. Solubility in the MEG + H_2O + Na_2CO_3 system at various temperatures as a function of solvent composition. The symbols are the experimental data from Gärtner et al.[29] and Oosterhof et al.,[30] and the lines are calculated using the MSE model with the parameters listed in Tables 3−7. The solid phases that are in equilibrium with the solutions are indicated in the legend.

H_2O + $NaHCO_3$ system in which the solubility shows an initial decrease at lower MEG concentrations followed by an increase at higher MEG contents after a minimum is reached. Also, such solubility minima have been consistently observed for this system at other temperatures. This is shown in Figure 8 at several temperatures from 20 to 90 °C.

A change in solvent composition frequently leads to a change in the degree of hydration of the precipitated solid phase. This is illustrated in Figure 9, which shows the solubilities in the MEG + H_2O + Na_2CO_3 system from 40 to 90 °C. The stable solid phase at these temperatures is $Na_2CO_3{\cdot}H_2O$ at lower MEG concentrations, whereas higher MEG concentrations favor the precipitation of anhydrous $Na_2CO_3(s)$. The transition concentration of MEG at which the stable solid phase changes from $Na_2CO_3{\cdot}H_2O$ to anhydrous $Na_2CO_3(s)$ decreases with temperature. The solubility curves that are calculated for this system are consistent with the data of Oosterhof et al.[30] and Gärtner et al.[29] The data points from Gärtner et al. are in fact smoothed values based on quadratic functions that were fit to the solubility data of Oosterhof et al. with correlation coefficients greater than 99.2%.[29] Because of the low solubilities at high MEG concentrations, the calculated solubility values deviate from the original data of Oosterhof et al. by as much as 30% in pure MEG. These deviations correspond to the reported accuracy of the measurements of Oosterhof et al.[30] The model represents the low solubilities at high MEG concentrations within the experimental uncertainty, as seen in Figure 9 in which solubilities are plotted on a logarithmic scale. Similar results are obtained for the MEG + H_2O + Na_2SO_4 system, as shown in Figure 10, where the calculated and experimental solubilities[13] are compared at various fixed MEG contents (from pure water to almost pure MEG) as a function of temperature. These results show that temperature has a much weaker effect on the solubility of Na_2SO_4 compared to the solvent composition. Evidently, it is the MEG content that causes a significant decrease in the solubility. The hydrated solid phase $Na_2SO_4{\cdot}10H_2O$ precipitates only at lower temperatures in water-dominated systems, whereas anhydrous $Na_2SO_4(s)$ is the solid phase that is in equilibrium with the solution over wide ranges of temperature and MEG concentration. The model accurately reproduces these phenomena.

In view of the importance of MEG-containing systems in oil and gas environments, the effect of temperature and MEG content on the solubility of acid gases and other gaseous components is of particular interest. This effect is illustrated in Figures 11−13. In Figure 11, the partial pressures of CO_2 and HCl in anhydrous MEG + CO_2 and MEG + HCl systems are shown as a function of the mole fractions of CO_2 or HCl at selected temperatures. Solubilities of HCl, H_2S, CO_2, and O_2 in pure liquid MEG are further compared in Figure 12 as functions of temperature at a total pressure of 1 atm. The solubility decreases with temperature, as expected, for all of the solutes. Furthermore, it is of particular interest to calculate the effect of varying solvent composition on the solubility of the gases. An example of such calculations is shown in Figure 13, which demonstrates the effects of MEG content and temperature on the solubility of O_2. The solubility increases with the MEG content at all temperatures, and this behavior is represented well within the experimental uncertainty.

Prediction of mineral scaling in the presence of MEG is one of the most important objectives of this study. Among the common scales, barite ($BaSO_4$) and calcite ($CaCO_3$) are of key importance. They often occur in brines dominated by NaCl, and their precipitation may be caused by the presence of MEG. Thus, their solubility behavior in relevant quaternary and quinary systems has been investigated. The results for the MEG + H_2O + $BaSO_4$ + NaCl system are illustrated in Figure 14 in which the experimental solubilities of $BaSO_4(s)$ are reproduced in MEG-containing mixtures in the presence of 1 and 3 mol (kg H_2O)$^{-1}$ of NaCl at 25 °C. Figure 15 shows the solubility of $CaCO_3(s)$ in the MEG + H_2O + $CaCO_3$ + NaCl + CO_2 system at 25, 60, and 80 °C with the NaCl content of 0.5 mol (kg solvent)$^{-1}$ and P_{CO_2} ~0.5−1 atm. The model accurately reproduces the decrease in the solubility with MEG concentration at all temperatures under these conditions.

In modeling the MEG systems containing carbonates and sulfates, it was necessary to introduce aqueous MEG-carbonate and MEG-sulfate complexes ($HOC_2H_4OCO_2^-$ and HO-

dx.doi.org/10.1021/ie4019353 | Ind. Eng. Chem. Res. 2013, 52, 15968−15987

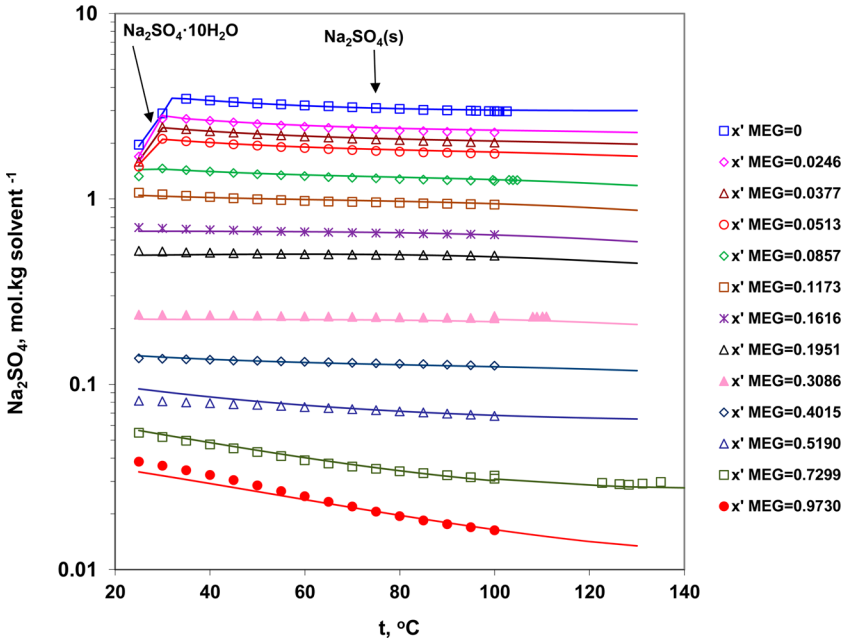

Figure 10. Solubility in the MEG + H_2O + Na_2SO_4 system at various solvent compositions (in mole fraction on a salt-free basis) as a function of temperature. The symbols are the experimental data from Vener and Thompson,[13] and the lines are calculated using the MSE model with the parameters listed in Tables 3−7.

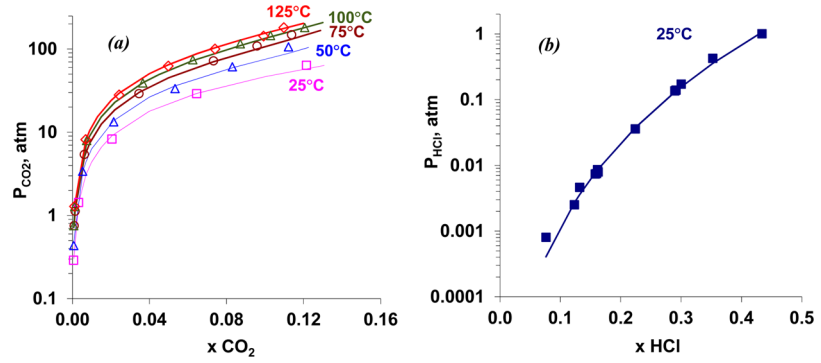

Figure 11. Partial pressure of CO_2 in the MEG + CO2 system (a) and partial pressure of HCl in the MEG + HCl system (b) as a function of the mole fraction of CO_2 or HCl, respectively. The symbols are the experimental data from Jou et al.[24] (for the CO_2 system) and O'Brien et al.[44] (for the HCl system). The lines are calculated using the MSE model with parameters listed in Tables 3−7.

$C_2H_4OHSO_4^{-2}$) to obtain the best fit to the experimental solubility data. In fact, the formation of MEG complexes with several inorganic ligands has been previously identified in the literature.[117,118] The appropriate thermochemical property values for these complexes have been determined in this study together with binary interaction parameters by regressing the experimental data. These values are included in Table 4.

pH in MEG + H_2O + Salt Systems. The presence of MEG not only affects the solubility of solids and VLE, but it also influences the solution pH. When the pH is calculated and compared with experimental results for mixed-solvent electrolyte systems such as the MEG + H_2O + salt mixtures, attention must be paid to the reference state that is used to define the pH scale. In particular, the experimental pH data for bicarbonate + MEG + water systems from Sandengen et al.[51] are based on calibration with a standard solution of potassium hydrogen phthalate in the same solvent. The reference pH values for standard solutions were previously determined for a range of ethylene glycol−water mixtures[52] and refitted by Sandengen et al.[51] The reference pH values were determined according to IUPAC's recommendation for mixed solvents[52,119] and do not refer to the absolute (universal) pH scale, which is defined on the basis of water as the reference state.

When using the water-based absolute scale, pH is calculated according to the definition

$$\mathrm{pH} = -\log(a_{H^+}) = -\log(m_{H^+}\gamma_{H^+}^{m,*}) \tag{11}$$

where $\gamma_{H^+}^{m,*}$ denotes the molality-based, unsymmetrically normalized activity coefficient. When pH is defined using the H_3O^+ ion instead of the H^+ ion, eq 11 can be rigorously rewritten as

$$\mathrm{pH} = -\log\left(\frac{a_{H_3O^+}}{a_{H_2O}}\right) = -\log\left(\frac{m_{H_3O^+}\gamma_{H_3O^+}^{m,*}}{a_{H_2O}}\right) \tag{12}$$

To transition from the universal H_2O-based scale to the scale that was used for the MEG-containing mixed-solvent solutions, the so-called "primary medium effect" (i.e., the Gibbs free energy of transfer of the proton from water to the mixed

dx.doi.org/10.1021/ie4019353 | Ind. Eng. Chem. Res. 2013, 52, 15968−15987

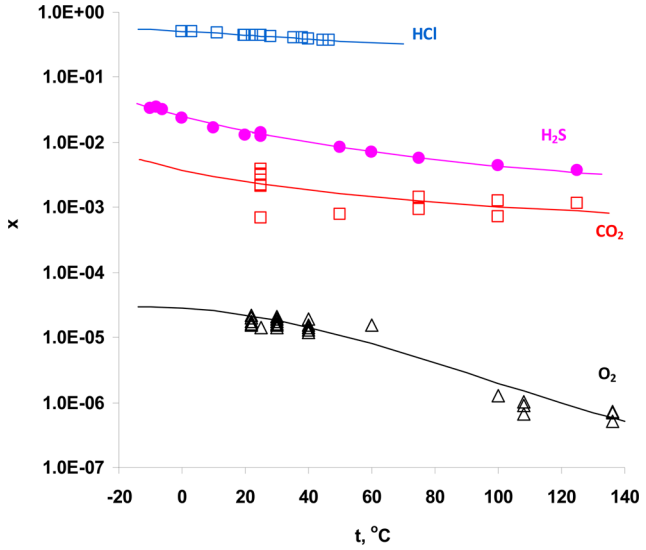

Figure 12. Solubilities of gases in liquid MEG as a function of temperature at 1 atm total pressure. The symbols are experimental data taken from the literature,[20,23−25,28,31,34,42,47] and the lines are calculated from the MSE model using the parameters given in Tables 3−7.

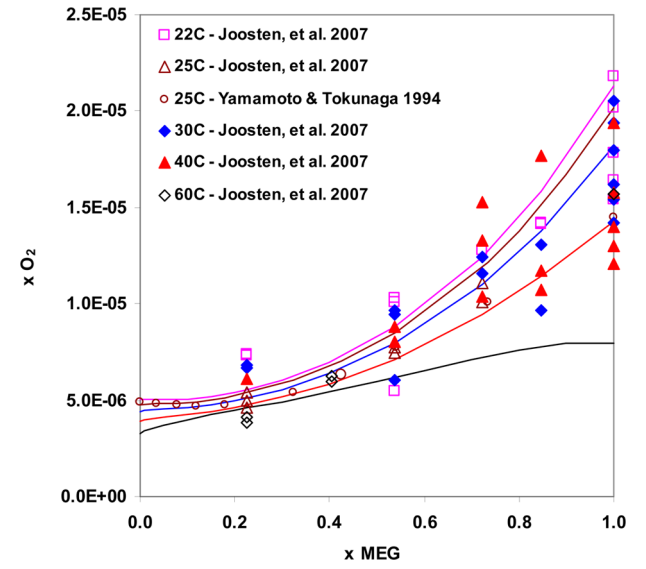

Figure 13. Solubility of O_2 in MEG + H_2O mixtures as a function of solvent composition at various temperatures. The symbols are the literature data,[22,47] and the lines are calculated from the MSE model using the parameters from Tables 3−7.

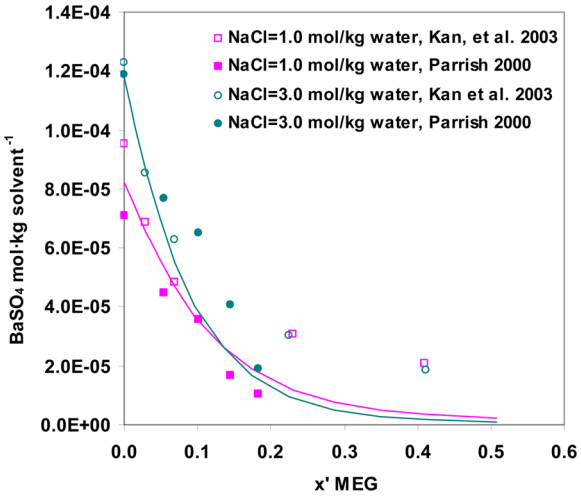

Figure 14. Solubilities of $BaSO_4$(s) in the MEG + H_2O + NaCl + $BaSO_4$ system as a function of solvent composition at 25 °C in the presence of 1.0 and 3.0 mol NaCl (kg H_2O)$^{-1}$. The symbols are the experimental data from Kan et al.[27] and Parrish,[40] and the lines are calculated using the MSE model with the parameters listed in Tables 3−7.

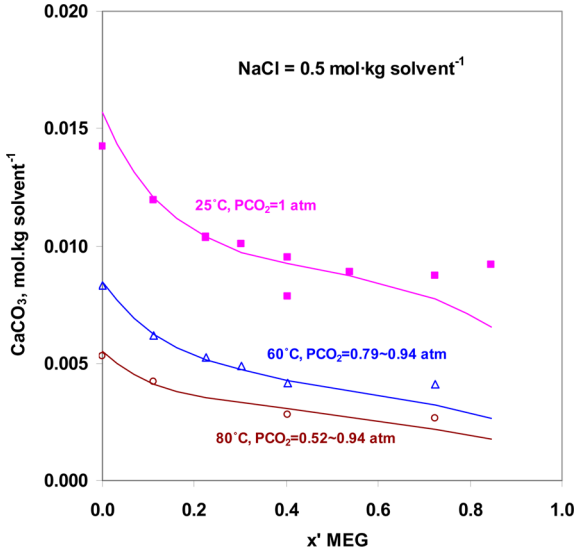

Figure 15. Solubilities of $CaCO_3$(s) in the MEG + H_2O + NaCl + $CaCO_3$ + CO_2 system as a function of solvent composition at 25, 60, and 80 °C in the presence of 0.5 mol NaCl (kg solvent)$^{-1}$. The symbols are the experimental data from Kaasa et al.,[26] and the lines are calculated using the MSE model with the parameters listed in Tables 3−7.

solvent) would need to be considered. This value can be related to activity coefficients and calculated on the basis of eq 10. When using molality-based activity coefficients, eq 10 can be rewritten as

$$\Delta_{tr}G^{\circ}_{H^+}(w \rightarrow s) = RT \ln \frac{M_s}{x^s_w M_w} \frac{\gamma^{m,*,s}_{H^+}}{\gamma^{m,*,w}_{H^+}} \quad (13)$$

where the superscripts w and s refer to water and the mixed solvent, respectively, and x^s_w is the mole fraction of water in the mixed solvent. This equation combines two effects: the effect of change in the molality base between water and a mixed solvent and the effect of differences in ion properties in the two media, which are represented by the activity coefficients. If the Gibbs energy of transfer of the hydrogen ion was available from an independent source, then the thermodynamic model could be constrained to represent the transition between the two pH scales. In fact, the MSE model accurately predicts the Gibbs energies of transfer of electrolytes (i.e., cation−anion combinations) on the basis of other kinds of data (such as solubility or VLE),[73] but a prediction of single-ion properties (such as pH) requires extra-thermodynamic assumptions and has to depend on the adopted reference state (i.e., a pH scale). Therefore, pH that is defined on the universal, or water-based, scale does not agree quantitatively with experimental data in solvents that are dominated by glycols or other components,

dx.doi.org/10.1021/ie4019353 | Ind. Eng. Chem. Res. 2013, 52, 15968−15987

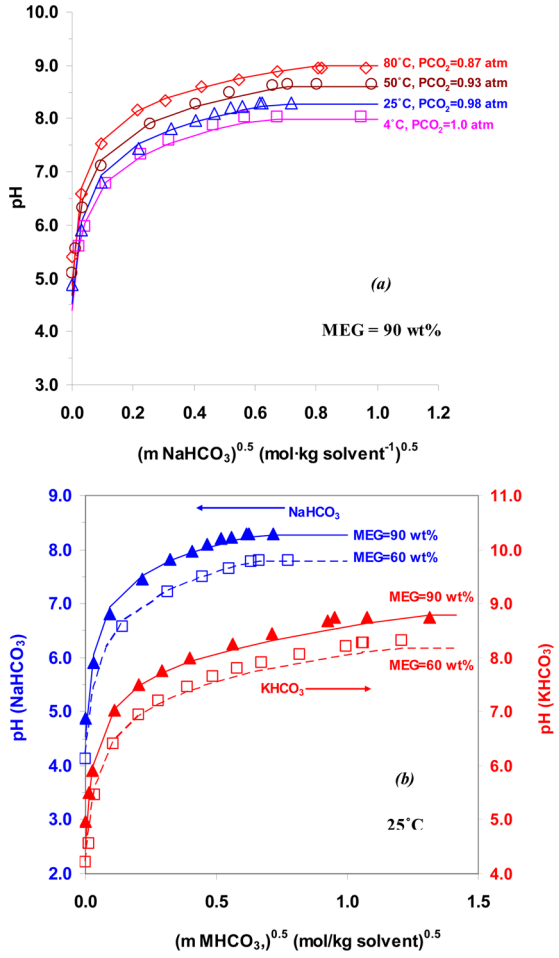

Figure 16. pH as a function of $NaHCO_3$ or $KHCO_3$ concentration (expressed as mol (kg solvent)$^{-1}$) in solutions of (a) MEG + H_2O + $NaHCO_3$ + CO_2 with 90 wt % of MEG (on a salt-free basis) at 4, 25, 60, and 80 °C and at the indicated PCO_2 and (b) MEG + H_2O + $MHCO_3$ + CO_2 (M═Na or K) with 60 and 90 wt % of MEG at 25 °C and P_{CO_2} ∼1 atm. The symbols are the experimental data from Sandengen et al.,[51] and the lines are calculated from the MSE model using the parameters given in Tables 3−7.

although the trends are the same. A systematic offset, which increases with glycol concentration, can be observed.[51]

Thus, rather than attempting to use eq 12 directly, a practical approximate approach is proposed here. This approach is based on the classical, concentration-based definition of pH[120]

$$\mathrm{pH} = -\log(c_{\mathrm{H}}) \tag{14}$$

where c_H is the molar concentration of the protonated solvent. For the MEG + water solutions, c_H must include all protonated forms of solvent components in order to reflect the reference state that is based on the mixed solvent. In MEG solutions, an additional protonated species, $HOC_2H_4OH_2^+$, is present together with the deprotonated one, $HOC_2H_4O^{1-}$, because of the self-dissociation of MEG (HOC_2H_4OH). In other words

$$2HOC_2H_4OH(aq) = HOC_2H_4OH_2^{+} + HOC_2H_4O^{-1} \tag{15}$$

Reaction 15 is analogous to the self-dissociation of H_2O:

$$2H_2O = H_3O^{+} + OH^{-} \tag{16}$$

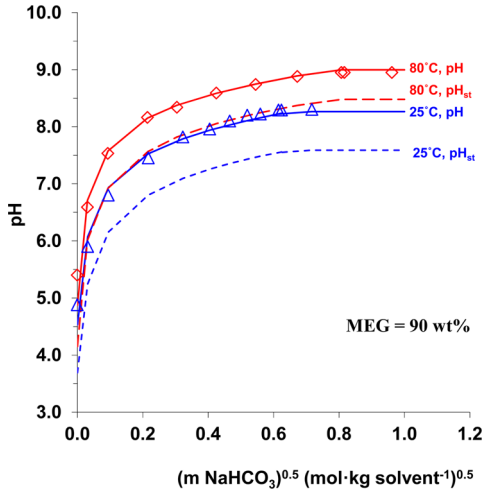

Figure 17. Comparison of pH values calculated using eq 17 (solid lines) with those obtained using the water-based scale (i.e., from eq 12) (pH_{sv}, dashed lines) in the system MEG + H_2O + $NaHCO_3$ + CO_2 with 90 wt % MEG (on a salt-free basis) at 25 and 80 °C. The symbols are the experimental data from Sandengen et al.[51]

The protonated species, $HOC_2H_4OH_2^+$, needs to be included in eq 14. Thus, the pH can be calculated as

$$\mathrm{pH} \cong -\log(c_{H_3O^+} + c_{HOC_2H_4OH_2^+}) \tag{17}$$

where both protonated solvent species (i.e., H_3O^+ and $HOC_2H_4OH_2^+$) contribute to the solution pH.

The standard-state thermochemical properties of $HOC_2H_4OH_2^+$ and $HOC_2H_4O^{1-}$ have not been found in the literature and have been estimated using the dissociation constant of reaction 15 as a function of temperature. The self-dissociation constant of MEG has been assumed to have a similar temperature dependence as that of water. In general, the dissociation constant of MEG follows the same pattern as that observed for alcohols.[121] The standard-state properties of the ionized MEG species are given in Table 4.

The pH values calculated using eq 17 are compared with the experimental data of Sandengen et al.[51] in Figure 16 for the MEG + H_2O + $KHCO_3$ + CO_2 and MEG + H_2O + $NaHCO_3$ + CO_2 systems. Figure 16 is plotted as a function of the square root of the bicarbonate concentration ($m^{1/2}$) to avoid the compression of results at low concentrations. The calculated and experimental pH increases with temperature (Figure 16a) and with the MEG concentration (Figure 16b). The results shown in Figure 16 indicate that the estimated standard-state properties of the dissociated MEG species are reasonable because they introduce an appropriate amount of the protonated species, $HOC_2H_4OH_2^+$. For comparison, Figure 17 includes the pH values obtained from both eqs 17 and 12. Clearly, a systematic offset is observed when the pH is calculated using the water-based scale (i.e., eq 12). The excellent agreement between the values obtained using eq 17 and the experimental data indicates that the approximate pH calculation scheme is physically meaningful.

Electrical Conductivity in MEG + H_2O + Salt Systems. The thermodynamic speciation results have been used as input for the calculation of electrical conductivity of the systems MEG + H_2O + NaCl, MEG + H_2O + $NaHCO_3$ and MEG + H_2O + NaCl + $NaHCO_3$. The parameters of the electrical conductivity model[100] have been adjusted to fit the experimental data. The electrical conductivity data in aqueous

dx.doi.org/10.1021/ie4019353 | Ind. Eng. Chem. Res. 2013, 52, 15968−15987

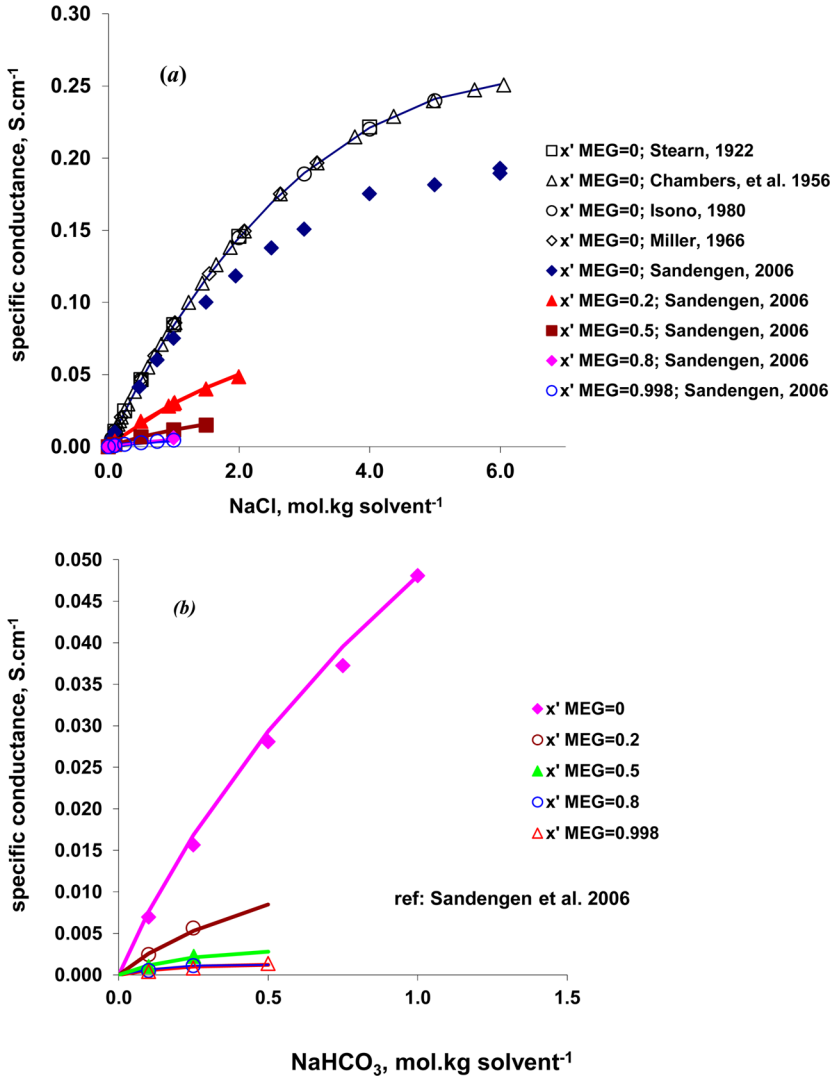

Figure 18. Electrical conductivity at various concentrations of MEG at 25 °C in the solutions of (a) MEG + H2O + NaCl and (b) MEG + H_2O + $NaHCO_3$. The symbols are experimental data from the literature,[70,123−126] and the lines are calculated from the electrical conductivity model[100] using the parameters given in Table S2.

solutions of NaCl and $NaHCO_3$ (i.e., for $x_{MEG} = 0$) have also been included in determining the model parameters so that the model can represent the electrical conductivity over the full range of solvent composition from pure water to pure MEG. The limiting ionic conductivities in pure MEG have been adopted from Marcus.[122] The electrical conductivity model parameters that have been determined in this study are provided in Table S2 in the Supporting Information. In Figure 18, the specific conductance of the MEG + H_2O + NaCl and MEG + H_2O + $NaHCO_3$ solutions is shown as a function of the salt concentration at various MEG mole fractions ranging from 0 to 1. The data in aqueous NaCl solutions (i.e., at $x_{MEG} = 0$) from Sandengen et al.[70] are significantly lower than those from other sources[123−126] at NaCl concentrations above approximately 2 *m* (Figure 18a). Thus, the data of Sandengen et al. were not used in determining the model parameters for solutions without MEG. However, these data are the only experimental source in the presence of MEG. In MEG-containing systems, they are all in the 2 *m* (mol/kg solvent) NaCl concentration region and show a systematic decrease in the conductivity with MEG content. Using the parameters determined in this study (Table S2), the model accurately represents the experimental data and the general trends of conductivity with MEG and salt concentrations. Similar results have also been obtained for the MEG + H_2O + $NaHCO_3$ system (Figure 18b). Results for the quaternary system MEG + H_2O + NaCl + $NaHCO_3$ are shown in Figure 19 for solutions with the concentration of $NaHCO_3$ fixed at 0.1 mol (kg solvent)$^{-1}$ (Figure 19a) and 0.25 mol (kg solvent)$^{-1}$ (Figure 19b). Here, the electrical conductivity increases with the NaCl concentration and decreases with the MEG content. Because of the presence of a significant amount of the complex species $HOC_2H_4OCO_2^-$ in the systems containing $NaHCO_3$ (especially at high MEG concentrations), a binary interaction between $HOC_2H_4OCO_2^-$ and Na^+ has been introduced to accurately reproduce the data.

These results show that the speciation obtained from the thermodynamic model is consistent with the observed electrical conductivity and makes it possible to represent simultaneously the chemical and phase equilibria and transport properties in mixed-solvent electrolyte systems.

dx.doi.org/10.1021/ie4019353 | *Ind. Eng. Chem. Res.* 2013, 52, 15968−15987

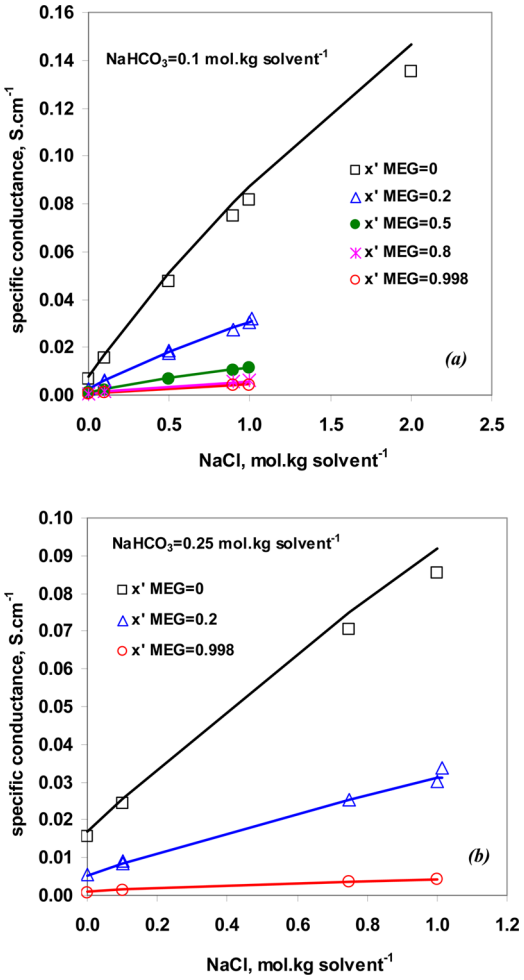

Figure 19. Electrical conductivity at various concentrations of MEG at 25 °C in the solutions of MEG + H_2O + NaCl + $NaHCO_3$ at fixed $NaHCO_3$ concentrations of (a) 0.1 and (b) 0.25 mol (kg solvent)$^{-1}$. The symbols are experimental data from the literature,[70] and the lines are calculated from the electrical conductivity model[100] using the parameters given in Table S2.

6. CONCLUSIONS

A comprehensive thermodynamic model has been applied to calculate various thermodynamic properties of mixtures containing monoethylene glycol as a solvent in addition to water. In particular, the model has been used to calculate the solubilities of solids and gases, vapor pressures, pH, heat capacities, and densities for various systems containing inorganic components in mixed MEG−H_2O solvents. The thermodynamic model has been shown to represent experimental data over wide ranges of temperature and concentration. Specifically, solubilities have been accurately reproduced in the full concentration range of the mixed solvent (i.e., for x_{MEG} from 0 to 1), with or without salt or acid gas components. The practical usefulness of the model has been demonstrated by predicting the solubility of common mineral scales (such as $BaSO_4$, $CaCO_3$, or NaCl) in multicomponent mixtures containing MEG. Moreover, pH of such systems can be predicted simultaneously with phase equilibria. In addition to the equilibrium thermodynamic properties of bulk solutions, transport properties and surface tension have been accurately reproduced using separate models with the same range of applicability. In particular, using the speciation obtained from the thermodynamic model, the electrical conductivity has been accurately computed for the MEG + H_2O + NaCl + $NaHCO_3$ solutions over wide ranges of solvent composition and salt concentration. Thus, the combined computational framework can be used to predict the bulk thermodynamic properties, surface tension and transport properties of multicomponent H_2O−MEG−Na−K−Ca−Ba−Cl−SO_4−CO_3−HCO_3−CO_2−H_2S−O_2 systems. This framework can be accessed through a software tool, OLI Analyzer Studio.[127]

■ ASSOCIATED CONTENT

Supporting Information

Brief summary of the models for thermal conductivity, viscosity, surface tension, and electrical conductivity and the parameters of these models for relevant MEG systems. This material is available free of charge via the Internet at http://pubs.acs.org.

■ AUTHOR INFORMATION

Corresponding Author

*Tel.: 1-973-539-4996. Fax: 1-973-539-5922. E-mail: pwang@olisystems.com.

Notes

The authors declare no competing financial interest.

■ REFERENCES

(1) Sloan, E. D. *Clathrate Hydrates of Natural Gases*, 2nd ed.; Marcel Dekker, Inc.: New York, 1998; Vol. 73, p 705.
(2) Gärtner, R. S.; Wilhelm, F. G.; Witkamp, G. J.; Wessling, M. Regeneration of Mixed Solvent by Electrodialysis: Selective Removal of Chloride and Sulfate. *J. Membr. Sci.* **2005**, *250*, 113−133.
(3) Oosterhof, H.; Witkamp, G. J.; van Rosmalen, G. M. Evaporative Crystallization of Anhydrous Sodium Carbonate at Atmospheric Conditions. *AIChE J.* **2001**, *47*, 2220−2225.
(4) Sokolov, N. M.; Tsygankova, L. N.; Zhavoronkov, N. M. Liquid-Vapor Phase Equilibrium in Water-Ethylene Glycol and Water-1,2-Propylene Glycol Systems at Various Pressures. *Teor. Osn. Khim. Tekhnol.* **1971**, *5*, 900−904.
(5) Chiavone-Filho, O.; Proust, P.; Rasmussen, P. Vapor-Liquid Equilibria of Glycol Ether + Water Systems. *J. Chem. Eng. Data* **1993**, *38*, 128−131.
(6) Trimble, H. M.; Potts, W. Glycol-Water Mixtures Vapor Pressure-Boiling Point-Composition Relations. *Ind. Eng. Chem.* **1935**, *27*, 66−68.
(7) Ogorodnikov, S. K.; Kogan, V. B.; Morozova, A. I. Liquid-Vapor Equilibrium in the System Ethylene Glycol-Water. *Zh. Prikl. Khim. (S.-Peterburg, Russ. Fed.)* **1962**, *35*, 685−687.
(8) Gonzalez, C.; Van Ness, H. C. Excess Thermodynamic Functions for Ternary Systems. 9. Total-Pressure Data and G^E for Water/Ethylene Glycol/Ethanol at 50 °C. *J. Chem. Eng. Data* **1983**, *28*, 410−412.
(9) Villamanan, M. A.; Gonzalez, C.; Van Ness, H. C. Excess Thermodynamic Properties for Water/Ethylene Glycol. *J. Chem. Eng. Data* **1984**, *29*, 427−429.
(10) Fox, J. M. *Vapor-Liquid Equilibrium Data for the Ethylene Glycol-Water System Saturated with Sodium Sulfate*. M.S. Thesis, University of Pennsylvenia, Philadelphia, PA, 1949.
(11) Zhou, Y.-H.; Li, S.-N.; Zhai, Q.-G.; Jiang, Y.-C.; Hu, M.-C. Compositions, Densities, and Refractive Indices for the Ternary Systems Ethylene Glycol + NaCl + H_2O, Ethylene Glycol + KCl + H_2O, Ethylene Glycol + RbCl + H_2O, and Ethylene Glycol + CsCl + H_2O at 298.15K. *J. Chem. Eng. Data* **2010**, *55*, 1289−1294.
(12) Zhou, Y.-H.; Li, S.-N.; Zhai, Q.-G.; Jiang, Y.-C.; Hu, M.-C. Solubilities, Densities, and Refractive Indices for the Ternary Systems Ethylene Glycol + MCl + H_2O (M═Na, K, Rb, Cs) at 15 and 35 °C. *J. Chem. Thermodyn.* **2010**, *42*, 764−772.

(13) Vener, R. E.; Thompson, A. R. Solubility and Density Isotherms for Sodium Sulfate-Ethylene Glycol-Water. *Ind. Eng. Chem.* **1949**, *41*, 2242−2247.
(14) Trimble, H. M. Solubilities of Salts in Ethylene Glycol and in Its Mixtures with Water. *Ind. Eng. Chem.* **1931**, *23*, 165−167.
(15) Trimble, H. M.; Ebert, P. F. The Effect of Ethylene Glycol upon the Activity of Sulfuric Acid in Aqueous Solutions. *J. Am. Chem. Soc.* **1933**, *55*, 958−968.
(16) Adamcová, Z. Solubility of KCl, KI, and KSCN in the Ternary System Electrolyte-Water-Ethylene Glycol (Dithylene Glycol, Triethylene Glycol). *Collect. Czech. Chem. Commun.* **1969**, *34*, 3149−3153.
(17) Masoudi, R.; Tohidi, B.; Danesh, A.; Todd, A. C.; Yang, J. Measurement and Prediction of Salt Solubility in the Presence of Hydrate Organic Inhibitors. *SPE Prod. Oper.* **2006**, *21*, 182−187.
(18) *Solubilities of Inorganic and Organic Compounds: Ternary and Multicomponent Systems of Inorganic Substances. Part 1−3*; Silcock, H. L., Ed.; Pergamon Press: New York, 1979; Vol. 3, p 3321.
(19) *Solubilities of Inorganic and Organic Compounds, Part 1−2*; Stephen, H., Stephen, T., Eds.; Pergamon Press: New York, 1964; Vol. 2, p 2053.
(20) Short, I.; Sahgai, A.; Hayduk, W. Solubility of Ammonia and Hydrogen Sulfide in Several Polar Solvents. *J. Chem. Eng. Data* **1983**, *28*, 63−66.
(21) Woods, E. J.; Zieger, M. A. J.; Gao, D. Y.; Critser, J. K. Equations for Obtaining Melting Points for the Ternary System Ethylene Glycol/Sodium Chloride/Water and Their Application to Cryopreservation. *Cryobiology* **1999**, *38*, 403−407.
(22) Yamamoto, H.; Tokunaga, J. Solubilities of Nitrogen and Oxygen in 1,2-Ethanediol + Water at 298.15 K and 101.33 kPa. *J. Chem. Eng. Data* **1994**, *39*, 544−547.
(23) Lenoir, J. Y.; Renault, P.; Renon, H. Gas Chromatographic Determination of Henry's Constants of 12 Gases in 19 Solvents. *J. Chem. Eng. Data* **1971**, *16*, 340−342.
(24) Jou, F.-Y.; Deshmukh, R. D.; Otto, F. D.; Mather, A. E. Vapor-Liquid Equilibria of H_2S and CO_2 and Ethylene Glycol at Elevated Pressures. *Chem. Eng. Commun.* **1990**, *87*, 223−231.
(25) Gerrard, W. Solubility of Hydrogen Sulphide, Dimethyl Ether, Methyl Chloride and Sulphur Dioxide in Liquids. The Prediction of Solubility of All Gases. *J. Appl. Chem. Biotechnol.* **1972**, *22*, 623−650.
(26) Kaasa, B.; Sandengen, K.; Østvold, T. Thermodynamic Predictions of Scale Potential, pH and Gas Solubility in Glycol Containing Systems. SPE 95075. In *SPE International Symposium on Oilfield Scale*, Aberdeen, U.K., May 11−12, 2005; pp 1−13.
(27) Kan, A. T.; Fu, G.; Tomson, M. B. Effect of Methanol and Ethylene Glycol on Sulfates and Halite Scale Formation. *Ind. Eng. Chem. Res.* **2003**, *42*, 2399−2408.
(28) Byeseda, J. J.; Deetz, J. A.; Manning, W. P. The OPTISOL Gas Sweetening Solvent. In *Proceedings of the Laurance Reid Gas Conditioning Conference*, Norman, OKMarch 4−6, 1985; University of Oklahoma: Norman, OK, 1985.
(29) Gärtner, R. S.; Seckler, M. M.; Witkamp, G.-J. Solid Phases and Their Solubilities in the System Na_2CO_3 + $NaHCO_3$ + Ethylene Glycol + Water from (50 to 90) °C. *J. Chem. Eng. Data* **2004**, *49*, 116−125.
(30) Oosterhof, H.; Witkamp, G. J.; van Rosmalen, G. M. Some Antisolvents for Crystallisation of Sodium Carbonate. *Fluid Phase Equilib.* **1999**, *155*, 219−227.
(31) Hayduk, W.; Malik, V. K. Density, Viscosity, and Carbon Dioxide Solubility and Diffusivity in Aqueous Ethylene Glycol Solutions. *J. Chem. Eng. Data* **1971**, *16*, 143−146.
(32) Kobe, K. A.; Mason, G. E. Aqueous Solutions of Alcohols as Confining Liquids for Gas Analysis. *Ind. Eng. Chem.* **1946**, *18*, 78−79.
(33) Won, Y. S.; Chung, D. K.; Mills, A. F. Density, Viscosity, Surface Tension, and Carbon Dioxide Solubility and Diffusivity of Methanol, Ethanol, Aqueous Propanol, and Aqueous Ethylene Glycol at 25 °C. *J. Chem. Eng. Data* **1981**, *26*, 140−141.
(34) Oyevaar, M. H.; Morssinkhof, R. W. J.; Westerterp, K. R. Density, Viscosity, Solubility, and Diffusivity of CO_2 and N_2O in Solutions of Diethanolamine in Aqueous Ethylene Glycol at 298 K. *J. Chem. Eng. Data* **1989**, *34*, 77−82.
(35) Kaminishi, G.-I.; Takano, S.; Yokoyama, C.; Takahashi, S.; Katsuhiko, T. Concentration of Triethylene Glycol, Diethylene Glycol and Ethylene Glycol in Supercritical Carbon Dioxide up to 16 MPa at 313.15 and 333.15 K. *Fluid Phase Equilib.* **1989**, *52*, 365−372.
(36) Masoudi, R.; Tohidi, B.; Anderson, R.; Burgass, R. W.; Yang, J. Experimental Measurement and Thermodynamic Modelling of Clathrate Hydrate Equilibria and Salt Solubility in Aqueous Ethylene Glycol and Electrolyte Solutions. *Fluid Phase Equilib.* **2004**, *219*, 157−163.
(37) Isbin, H. S.; Kobe, K. A. The Solubility of Some Salts in Ethylenediamine, Monoethanolamine and Ethylene Glycol. *J. Am. Chem. Soc.* **1945**, *67*, 464−465.
(38) Kraus, K. A.; Raridon, R. J.; Baldwin, W. H. Properties of Organic-Water Mixtures. I. Activity Coefficients of Sodium Chloride, Potassium Chloride, and Barium Nitrate in Saturated Water Mixtures of Glycol, Glycerol, and Their Acetates. Model Solutions for Hyperfiltration Membranes. *J. Phys. Chem.* **1964**, *68*, 2571−2576.
(39) Baldwin, W. H.; Raridon, R. J.; Kraus, K. A. Properties of Organic-Water Mixtures. X. Activity Coefficients of Sodium Chloride at Saturation in Water Mixtures of Polyglycols and Polyglycol Ethers at 50°C. *J. Phys. Chem.* **1969**, *73*, 3417−3420.
(40) Parrish, W. R. *Thermodynamic Inhibitors in Brines*; DeepStar Project CTR 4210 Report: Houston, TX, 2000
(41) Parrish, W. R.; Allred, G. C. *Methanol and Ethylene Glycol Mixtures Containing Salts. Phase II: Data for Improving Hydrate Prediction Methods*; DeepStar Project CTR 5205 Report: Houston, TX, 2002
(42) Gerrard, W.; Macklen, E. D. Solubility of Hydrogen Halides in Organic Compounds Containing Oxygen. IV. Solubility of Hydrogen Chloride in Glycols and Ethers. *J. Appl. Chem. Biotechnol.* **1960**, *10*, 57−62.
(43) Matuszak, M. P.; Bartlesville, O. *Recovery of Hydrogen Halides*. Patent No. 2520947, 1950.
(44) O'Brien, S. J.; Kenny, C. L.; Zuercher, R. A. The Partial Pressure of Hydrogen Chloride from its Solutions in Ethylene Glycol and Other Solvents at 25°. *J. Am. Chem. Soc.* **1939**, *61*, 2504−2507.
(45) Masoudi, R.; Tohidi, B.; Danesh, A.; Todd, A. C.; Anderson, R.; Burgass, R. W.; Yang, J. Measurement and Prediction of Gas Hydrate and Hydrated Salt Equilibria in Aqueous Ethylene Glycol and Electrolyte Solutions. *Chem. Eng. Sci.* **2005**, *60*, 4213−4224.
(46) Kobe, K. A.; Stong, J. P. The Ternary Systems Ethylene Glycol−Potassium Carbonate−Water and Dioxane−Potassium Carbonate−Water. *J. Phys. Chem.* **1940**, *44*, 629−633.
(47) Joosten, M. W.; Seiersten, M.; Tier, B.; Wintermark, C. Materials Considerations for MEG (Mono Ethylene Glycol) Reclaim Systems. Paper No. 07116. In *NACE Corrosion Conference and Expo*, Nashville, TN, March 11−15, 2007; Curran Associates: Red Hook, NY, 2007.
(48) Armstrong, H. E.; Eyre, J. V. Studies of the Processes Operative in Solutions. XXV. The Influence of Non-Electrolytes on Solubility. The Nature of Processes of Dissolution and Precipitation. *Proc. R. Soc. A* **1913**, *88*, 234−245.
(49) Chiavone-Filho, O.; Rasmussen, P. Solubilities of Salts in Mixed Solvents. *J. Chem. Eng. Data* **1993**, *38*, 367−369.
(50) Fox, J. J.; Gauge, A. J. H. The Solubility of Potassium Sulphate in Concentrated Aqueous Solutions of Non-Electrolytes. *J. Chem. Soc., Trans.* **1910**, *97*, 377−385.
(51) Sandengen, K.; Kaasa, B.; Østvold, T. pH Measurements in Monoethylene Glycol (MEG) + Water Solutions. *Ind. Eng. Chem. Res.* **2007**, *46*, 4734−4739.
(52) Mussini, T.; Longhi, P.; Marcolungo, I.; Mussini, P. R.; Rondinini, S. Status and Problems of Standardization of pH Scales for Controls in Different Media. Reference Value Standards in Ethylene Glycol/Water Mixed Solvents. *Fresenius' J. Anal. Chem.* **1991**, *339*, 608−612.
(53) Yang, C.; Ma, P.; Jing, F.; Tang, D. Excess Molar Volumes, Viscosities, and Heat Capacities for the Mixtures of Ethylene Glycol +

Water from 273.15 K to 353.15K. *J. Chem. Eng. Data* **2003**, *48*, 836−840.
(54) Nan, Z.; Liu, B.; Tan, Z. Calorimetric Investigation of Excess Molar Heat Capacities for Water + Ethylene Glycol from T=273.15 to T=373.15K. *J. Chem. Thermodyn.* **2002**, *34*, 915−926.
(55) Egorov, G. I.; Makarov, D. M.; Kolker, A. M. Volumetric Properties of the Water-Ethylene Glycol Mixtures in the Temperature Range 278−333.15 K at Atmospheric Pressure. *Russ. J. Gen. Chem.* **2010**, *80*, 1577−1585.
(56) Lee, H.; Hong, W.-H. Excess Volumes of Binary and Ternary Mixtures of Water, Methanol, and Ethylene Glycol. *J. Chem. Eng. Data* **1990**, *35*, 371−374.
(57) Zhang, J.-B.; Zhang, P.-Y.; Ma, K.; Han, F.; Chen, G.-H.; Wei, X.-H. Hydrogen Bonding Interactions Between Ethylene Glycol and Water: Density, Excess Molar Volume, and Spectral Study. *Sci. China, Ser. B: Chem.* **2008**, *51*, 420−426.
(58) Kalies, G.; Brauer, P.; Schmidt, A.; Messow, U. Calculation and Prediction of Adsorption Excesses on the Ternary Liquid Mixture/Air Interface from Surface Tension Measurements. *J. Colloid Interface Sci.* **2002**, *247*, 1−11.
(59) Nakanishi, K.; Matsumoto, T.; Hayatsu, M. Surface Tension of Aqueous Solutions of Some Glycols. *J. Chem. Eng. Data* **1971**, *16*, 44−45.
(60) Habrdova, K.; Hovorka, K.; Bartovska, A. Concentration Dependence of Surface Tension for Very Dilute Aqueous Solutions of Organic Nonelectrolytes. *J. Chem. Eng. Data* **2004**, *49*, 1003−1007.
(61) Hoke, B. C.; Chen, J. C. Binary Aqueous Organic-Surface Tension Temperature-Dependence. *J. Chem. Eng. Data* **1991**, *36*, 322−326.
(62) Horibe, A.; Fukusako, S.; Yamada, M. Surface Tension of Low-Temperature Aqueous Solutions. *Int. J. Thermophys.* **1996**, *17*, 483−493.
(63) Sun, T.; Teja, A. S. Density, Viscosity, and Thermal Conductivity of Aqueous Ethylene, Diethylene, and Triethylene Glycol Mixtures Between 290 and 450K. *J. Chem. Eng. Data* **2003**, *48*, 198−202.
(64) Sesta, B.; Berardelli, M. L. Alkali-Nitrate Interactions in Water-Ethylene-Glycol Mixtures. Conductometric Measurements at 25°C. *Electrochim. Acta* **1972**, *17*, 915−919.
(65) Usmanov, I. U.; Salikhov, A. S. The Concentration Variation of the Thermal Conductivities of Certain Aqueous Solutions of Organic Liquids. *Russ. J. Phys. Chem.* **1977**, *51*, 1488−1489.
(66) Vanderkooi, W. N.; Hildenbrandt, D. L.; Stull, D. R. Liquid Thermal Conductivities. The Apparatus, Values for Several Glycols and Their Aqueous Solutions, and Five High Molecular Weight Hydrocarbons. *J. Chem. Eng. Data* **1967**, *12*, 377−379.
(67) Bohne, D.; Fischer, S.; Obermeier, E. Thermal Conductivity, Density, Viscosity, and Prandtl-Numbers of Ethylene Glycol-Water Mixtures. *Bunsen-Ges. Phys. Chem., Ber.* **1984**, *88*, 739−742.
(68) Assael, M. J.; Charitidou, E.; Avgoustiniatos, S.; Wakeham, W. A. Absolute Measurements of the Thermal Conductivity of Alkane-Glycols with Water. *Int. J. Thermophys.* **1989**, *10*, 1127−1140.
(69) Bogacheva, I. S.; Zemdikhanov, K. B.; Mukhamedzyanov, G. K.; Sadykov, A. K.; Usmanov, A. G. Thermal Conductivity of Solutions of Some Organic Liquids. *Russ. J. Phys. Chem.* **1980**, *54*, 838−839.
(70) Sandengen, K.; Kaasa, B. Estimation of Monoethylene Glycol (MEG) Content in Water + MEG + NaCl + $NaHCO_3$ Solutions. *J. Chem. Eng. Data* **2006**, *51*, 443−447.
(71) Fosbøl, P. L.; Thomsen, K.; Stenby, E. H. Modeling of the Mixed Solvent Electrolyte System CO_2−Na_2CO_3−$NaHCO_3$−Monoethylene Glycol−Water. *Ind. Eng. Chem. Res.* **2009**, *48*, 4565−4578.
(72) Anderko, A.; Wang, P.; Rafal, M. Electrolyte Solutions: from Thermodynamic and Transport Property Models to the Simulation of Industrial Processes. *Fluid Phase Equilib.* **2002**, *194*, 123−142.
(73) Wang, P.; Anderko, A.; Young, R. D. A Speciation-Based Model for Mixed-Solvent Electrolyte Systems. *Fluid Phase Equilib.* **2002**, *203*, 141−176.
(74) Wang, P.; Springer, R. D.; Anderko, A.; Young, R. D. Modeling Phase Equilibria and Speciation in Mixed-Solvent Electrolyte Systems. *Fluid Phase Equilib.* **2004**, *222*, 11−17.
(75) Wang, P.; Anderko, A.; Springer, R. D.; Young, R. D. Modeling Phase Equilibria and Speciation in Mixed-Solvent Electrolyte Systems: II. Liquid-Liquid Equilibria and Properties of Associating Electrolyte Solutions. *J. Mol. Liq.* **2006**, *125*, 37−44.
(76) Wang, P.; Anderko, A.; Springer, R. D.; Lencka, M. M. Speciation and Phase Behavior in Mixed Solvent Electrolyte Solutions: Thermodynamic Modeling. In *Proceedings: 17th International Symposium on Industrial Crystallization*; Jansens, J. P., Ulrich, J., Eds.; EFCE: Maastricht, The Netherlands, 2008; Vol. *1*.
(77) Wang, P.; Anderko, A.; Young, R. D.; Springer, R. D. In *Computational Analysis in Hydrometallurgy: 35th Annual Hydrometallurgy Meeting*; Dixon, D. G., Dry, M. J., Eds.; Canadian Institute of Mining, Metallurgy and Petroleum: Montreal, Canada, 2005; pp 259−273.
(78) Gruszkiewicz, M. S.; Palmer, D. A.; Springer, R. D.; Wang, P. M.; Anderko, A. Phase Behavior of Aqueous Na-K-Mg-Ca-Cl-NO_3 mixtures: Isopiestic Measurements and Thermodynamic Modeling. *J. Solution Chem.* **2007**, *36*, 723−765.
(79) Kosinski, J. J.; Wang, P. M.; Springer, R. D.; Anderko, A. Modeling Acid-Base Equilibria and Phase Behavior in Mixed-Solvent Electrolyte Systems. *Fluid Phase Equilib.* **2007**, *256*, 34−41.
(80) Liu, H.; Papangelakis, V. G. Thermodynamic Equilibrium of the O_2-$ZnSO_4$-H_2SO_4-H_2O System from 25 to 250 °C. *Fluid Phase Equilib.* **2005**, *234*, 122−130.
(81) Liu, H.; Papangelakis, V. G. Solubility of Pb(II) and Ni(II) in Mixed Sulfate−Chloride Solutions with the Mixed Solvent Electrolyte Model. *Ind. Eng. Chem. Res.* **2006**, *45*, 39−47.
(82) Azimi, G.; Papangelakis, V. G.; Dutrizac, J. E. Modelling of Calcium Sulphate Solubility in Concentrated Multi-Component Sulphate Solutions. *Fluid Phase Equilib.* **2007**, *260*, 300−315.
(83) Azimi, G.; Papangelakis, V. G.; Dutrizac, J. E. Development of an MSE-Based Chemical Model for the Solubility of Calcium Sulphate in Mixed Chloride-Sulphate Solutions. *Fluid Phase Equilib.* **2008**, *266*, 172−186.
(84) Wang, P.; Kosinski, J. J.; Lencka, M. M.; Anderko, A.; Springer, R. D. Thermodynamic Modeling of Boric Acid and Selected Metal Borate Systems. *Pure Appl. Chem.* [Online early access]. DOI: 10.1351/PAC-CON-12-07-09. Published Online: Jan 26, **2013**.
(85) Wang, P.; Anderko, A. Modeling Chemical Equilibria, Phase Behavior, and Transport Properties in Ionic Liquid Systems. *Fluid Phase Equilib.* **2011**, *302*, 74−82.
(86) Pitzer, K. S. *Activity Coefficients in Electrolyte Solutions*, 2nd ed.; CRC Press: Boca Raton, FL, 1991.
(87) Abrams, D. S.; Prausnitz, J. M. Statistical Thermodynamics of Liquid Mixtures - New Expressions for Excess Gibbs Energy of Partly or Completely Miscible Systems. *AIChE J.* **1975**, *21*, 116−128.
(88) Helgeson, H. C.; Kirkham, D. H.; Flowers, G. C. Theoretical Prediction of the Thermodynamic Behavior of Aqueous Electrolytes at High Pressures and Temperatures. I Summary of the Thermodynamic/Electrostatic Properties of the Solvent. *Am. J. Sci.* **1974**, *274*, 1089−1198.
(89) Helgeson, H. C.; Kirkham, D. H.; Flowers, G. C. Theoretical Prediction of the Thermodynamic Behavior of Aqueous Electrolytes at High Pressures and Temperatures. III Equation of State for Aqueous Species at Infinite Dilution. *Am. J. Sci.* **1976**, *276*, 97−240.
(90) Helgeson, H. C.; Kirkham, D. H.; Flowers, G. C. Theoretical Prediction of the Thermodynamic Behavior of Aqueous Electrolytes at High Pressures and Temperatures. IV. Calculation of Activity Coefficients, Osmotic Coefficients, and Apparent Molal and Standard and Relative Partial Molal Properties to 5 kb and 600°C. *Am. J. Sci.* **1981**, *281*, 1241−1516.
(91) Shock, E. L.; Helgeson, H. C. Calculation of the Thermodynamic and Transport Properties of Aqueous Species at High Pressures and Temperatures: Correlation Algorithms for Ionic Species and Equation of State Predictions to 5 kb and 1000°C. *Geochim. Cosmochim. Acta* **1988**, *52*, 2009−2036.

(92) Sverjensky, D. A.; Shock, E. L.; Helgeson, H. C. Prediction of the Thermodynamic Properties of Aqueous Metal Complexes to 1000°C and 5 kb. *Geochim. Cosmochim. Acta* **1997**, *61*, 1359−1412.
(93) Shock, E. L.; Helgeson, H. C.; Sverjensky, D. A. Calculation of the Thermodynamic and Transport Properties of Species at High Pressures and Temperatures: Standard Partial Molar Properties of Inorganic Neutral Species. *Geochim. Cosmochim. Acta* **1989**, *53*, 2157−2183.
(94) Soave, G. Equilibrium Constants from a Modified Redlich-Kwong Equation of State. *Chem. Eng. Sci.* **1972**, *27*, 1197−1203.
(95) Springer, R. D.; Wang, Z.; Anderko, A.; Wang, P.; Felmy, A. R. A Thermodynamic Model for Predicting Mineral Reactivity in Supercritical Carbon Dioxide: I. Phase Behavior of Carbon Dioxide−Water−Chloride Salt Systems Across the H_2O-Rich to the CO_2-Rich Regions. *Chem. Geol.* **2012**, *322*−*323*, 151−171.
(96) Zemaitis, J. F.; Clark, D. M.; Rafal, M.; Scrivner, N. C. *Handbook of Aqueous Electrolyte Thermodynamics*; American Institute of Chemical Engineers: New York, 1986.
(97) Rafal, M.; Berthold, J. W.; Scrivner, N. C.; Grise, S. L. Models for Electrolyte Solutions. In *Models for Thermodynamic and Phase Equilibria Calculations*; Sandler, S. I., Ed.; Marcel Dekker: New York, 1994.
(98) Wang, P.; Anderko, A. Modeling Thermal Conductivity of Concentrated and Mixed-Solvent Electrolyte Systems. *Ind. Eng. Chem. Res.* **2008**, *47*, 5698−5709.
(99) Wang, P.; Anderko, A.; Young, R. D. Modeling Viscosity of Concentrated and Mixed-Solvent Electrolyte Systems. *Fluid Phase Equilib.* **2004**, *226*, 71−82.
(100) Wang, P.; Anderko, A.; Young, R. D. Modeling Electrical Conductivity in Concentrated and Mixed-Solvent Electrolyte Solutions. *Ind. Eng. Chem. Res.* **2004**, *43*, 8083−8092.
(101) Wang, P.; Anderko, A.; Young, R. D. Modeling Surface Tension of Concentrated and Mixed-Solvent Electrolyte Systems. *Ind. Eng. Chem. Res.* **2011**, *50*, 4086−4098.
(102) Anderko, A.; Lencka, M. M. Computation of Electrical Conductivity of Multicomponent Aqueous Systems in Wide Concentration and Temperature Ranges. *Ind. Eng. Chem. Res.* **1997**, *36*, 1932−1943.
(103) Lencka, M. M.; Anderko, A.; Sanders, S. J.; Young, R. D. Modeling Viscosity of Multicomponent Electrolyte Solutions. *Int. J. Thermophys.* **1998**, *19*, 367−378.
(104) Wang, P.; Anderko, A. Modeling Interfacial Tension in Liquid-Liquid Systems Containing Electrolytes. *Ind. Eng. Chem. Res.* **2013**, *52*, 6822−6840.
(105) Wang, P.; Anderko, A. Modeling Self-Diffusion in Mixed-Solvent Electrolyte Solutions. *Ind. Eng. Chem. Res.* **2003**, *42*, 3495−3504.
(106) Anderko, A.; Lencka, M. M. Modeling Self-Diffusion in Multicomponent Aqueous Electrolyte Systems in Wide Concentration Ranges. *Ind. Eng. Chem. Res.* **1998**, *37*, 2878−2888.
(107) Wang, P.; Anderko, A. Modeling Thermal Conductivity of Electrolyte Mixtures in Wide Temperature and Pressure Ranges: Seawater and Its Main Components. *Int. J. Thermophys.* **2012**, *33*, 235−258.
(108) *Glycols*; Curme, G. O., Ed.; Reinhold Publishing Corporation: New York, 1953.
(109) Horstmann, S.; Gardeler, H.; Wilken, M.; Fischer, K.; Gmehling, J. Isothermal Vapor-Liquid Equilibrium and Excess Enthalpy Data for the Binary Systems Water + 1,2-Ethanediol and Propene + Acetophenone. *J. Chem. Eng. Data* **2004**, *49*, 1508−1511.
(110) Daubert, T. E.; Danner, R. P. *Physical and Thermodynamic Properties of Pure Chemicals*; Hemisphere Publishing Corp.: New York, 1989.
(111) Cordray, D. R.; Kaplan, L. R.; Woyciesjes, P. M.; Kozak, T. F. Solid-Liquid Phase Diagram for Ethylene Glycol + Water. *Fluid Phase Equilib.* **1996**, *117*, 146−152.
(112) Ross, H. K. Cryoscopic Studies: Concentrated Solutions of Hydroxy Compounds. *Ind. Eng. Chem.* **1954**, *46*, 601−610.
(113) Liu, J.; Cheng, X.; Pu, J.; Zhang, J.; Liu, J.; Wang, X. Experimental Study of the Electrical Characteristics of Ethylene Glycol/Water Mixtures in the Microsecond Regime. *IEEE Electr. Insul. Mag.* **2007**, *23*, 20−25.
(114) Weast, R. C.; Lide, D. R. *CRC Handbook of Chemistry and Physics*, 70th ed.; CRC Press, Inc.: Boca Raton, FL, 1990.
(115) Morénas, M.; Douhéret, G. Thermodynamic Behaviour of Some Glycol−Water Mixtures. Excess and Partial Volumes. *Thermochim. Acta* **1978**, *25*, 217−224.
(116) Iulian, O.; Ciocîrlan, O. Viscosity and Density of Systems with Water, 1,4-Dioxane and Ethylene Glycol Between (293.15 and 313.15) K. I. Binary Systems. *Rev. Roum. Chim.* **2010**, *55*, 45−53.
(117) Knetsch, D.; Groeneveld, W. L. Alcohols as Ligands: Part IV. Complexes of Ethylene Glycol with Some Metal(II) Sulfates and Nitrates. *Recl. Trav. Chim. Pays-Bas* **1973**, *92*, 855−864.
(118) Knetsch, D.; Groeneveld, W. L. Alcohol as Ligands. III. Complexes of Ethylene Glycol with Some Divalent Metal Halides. *Inorg. Chim. Acta* **1973**, *7*, 81−87.
(119) Mussini, P. R.; Mussini, T.; Rondinini, S. Reference Value Standards and Primary Standards for pH Measurements in D_2O and Aqueous-Organic Solvent Mixtures: New Accession and Assessments. *Pure Appl. Chem.* **1997**, *69*, 1007−1014.
(120) Sørensen, S. P. L. Enzyme Studies II. The Measurement and Meaning of Hydrogen Ion Concentration in Enzymatic Processes. *Biochem. Z.* **1909**, *21*, 131−200.
(121) Ueno, M.; Matsukawa, K.; Tsuchihashi, N.; Shimizu, K. Pressure Effect on Proton Jumps in t-Butyl Alcohol-Water Mixtures at 25°C. *Bull. Chem. Soc. Jpn.* **1991**, *64*, 931−937.
(122) Marcus, Y. *Ion Properties*; Marcel Dekker Inc.: New York, 1997.
(123) Stearn, A. E. Ionic Equilibria of Strong Electrolytes. *J. Am. Chem. Soc.* **1922**, *44*, 670−678.
(124) Chambers, J. F.; Stokes, J. M.; Stokes, R. H. Conductances of Concentrated Aqueous Sodium and Potassium Chloride Solutions at 25°C. *J. Phys. Chem.* **1956**, *60*, 985−986.
(125) Isono, T. Measurements of Density, Viscosity and Electric Conductivity of Concentrated Aqueous Electrolyte Solutions. I. LiCl, NaCl, KCl, RbCl, CsCl, $MgSO_4$, $ZnSO_4$ and $NiSO_4$. *Rikagaku Kenkyusho Hokoku* **1980**, *56*, 103−114.
(126) Miller, D. G. Application of Irreversible Thermodynamics to Electrolyte Solutions. I. Determination of Ionic Transport Coefficients l_{ij} for Isothermal Vector Transport Processes in Binary Electrolyte Systems. *J. Phys. Chem.* **1966**, *70*, 2639−2659.
(127) *Analyzer Studio 9.0*; OLI Systems, Inc.: Cedar Knolls, NJ; http://www.olisystems.com.
(128) Kubaschewski, O.; Ünal, H. An Empirical Estimation of the Heat Capacities of Inorganic Compounds. *High Temp. − High Pressures* **1977**, *9*, 361−365.
(129) Gurvich, L. V.; Veyts, I. V.; Alcock, C. B. *Thermodynamic Properties of Individual Substances*, 4th ed; Hemisphere Publishing Corporation: New York, 1989.
(130) Wagman, D. D.; Evans, W. H.; Parker, V. B.; Schumm, R. H.; Halow, I.; Bailey, S.; Churney, K. L.; Nuttal, R. L. The NBS Tables of Chemical Thermodynamic Properties. Selected Values for Inorganic and C1 and C2 Organic Substances in SI Units, Supplement 2. *J. Phys. Chem. Ref. Data* **1982**, *11*, 2−392.
(131) Majzlan, J.; Navrotsky, A.; Neil, J. M. Energetics of Anhydrite, Barite, Celestine, and Anglesite: A High-Temperature and Differential Scanning Calorimetry Study. *Geochim. Cosmochim. Acta* **2002**, *66*, 1839−1850.
(132) Glushko, V. P.; Gurvich, L. V.; Bergman, G. A.; Veyts, I. V.; Medvedev, V. A.; Kchachkurusov, G. A.; Yungman, B. S. *Thermodynamic Properties of Individual Substances*. Nauka: Moscow, 1982; Vol. 4.
(133) Hurst, J. E.; Harrison, B. K. Estimation of Liquid and Solid Heat Capacities Using a Modified Kopp's Rule. *Chem. Eng. Commun.* **1992**, *112*, 21−30.